ORNL/TM-2023/2923

Uncertainty Quantification of Fuel Inhomogeneity in Low-enriched Uranium Silicide High Flux Isotope Reactor Design

Donny Hartanto
David Chandler
Jin Whan Bae
Benjamin R. Betzler
Kevin Burg
Carol Sizemore

November 2023

OAK RIDGE National Laboratory

ORNL IS MANAGED BY UT–BATTELLE, LLC, FOR THE U.S. DEPARTMENT OF ENERGY

ORNL/TM-2023/2923

Nuclear Energy and Fuel Cycle Division

UNCERTAINTY QUANTIFICATION OF FUEL INHOMOGENEITY IN LOW-ENRICHED URANIUM SILICIDE HIGH FLUX ISOTOPE REACTOR DESIGN

Donny Hartanto
David Chandler
Jin Whan Bae
Benjamin R. Betzler
Kevin Burg
Carol Sizemore

Date Published: November 2023

Prepared by
OAK RIDGE NATIONAL LABORATORY
Oak Ridge, TN 37831-6283
managed by
UT-Battelle, LLC
for the
US DEPARTMENT OF ENERGY
under contract DE-AC05-00OR22725

CONTENTS

LIST OF FIGURES

LIST OF TABLES

ABBREVIATIONS

BOC	beginning-of-cycle
DOE	US Department of Energy
HEU	highly enriched uranium
HFIR	High Flux Isotope Reactor
IFE	inner fuel element
LEU	low-enriched uranium
M3	Office of Material Management and Minimization
NNSA	National Nuclear Security Administration
OFE	outer fuel element
ORNL	Oak Ridge National Laboratory

ACKNOWLEDGMENTS

This work is supported by the Office of Material Management and Minimization, National Nuclear Security Administration, US Department of Energy. This report was authored by UT-Battelle LLC, under contract DE AC05 00OR22725 with the US DOE. The authors would like to thank C. J. Hurt and Valerie Fudurich for the technical reviews of this paper.

ABSTRACT

This work evaluates the effect of fuel inhomogeneity uncertainty on Oak Ridge National Laboratory (ORNL)'s HFIR core performance to support the low-enriched uranium (LEU) conversion program. Fuel inhomogeneity is manufacturing-induced non-uniform uranium distribution in the involute fuel element (i.e., deviation from the nominal uranium distribution). Therefore, analyzing the fuel inhomogeneity impact in the HFIR LEU core is essential to assess the HFIR LEU performance and safety sensitivity to the homogeneity distributions. However, inhomogeneity distribution data from LEU U_3O_8-Al fuel element manufacture is still unavailable. Thus, this work leverages proposed conservative highly enriched uranium HEU U_3O_8-Al fuel element inhomogeneity profiles and tolerances to create five representative LEU inhomogeneity profiles. The effect of fuel inhomogeneity is assessed for the proposed low-density U_3Si_3-Al core design, and several key parameters are evaluated, including multiplication factor (i.e., k_{eff}), cold source moderator vessel cold neutron flux and cold-to-total neutron flux ratio, ^{252}Cf target thermal neutron flux, flux trap fast neutron flux, reflector fast neutron flux, and fission rate density distribution. This work finds that the uncertainty caused by the fuel inhomogeneity reduces the averaged reactivity and the flux at target by 0.18% and 0.43%, respectively, which can be considered negligible. In addition, the change of the fission density due to the fuel inhomogeneity is still within the assumed safety analyses tolerances.

1. INTRODUCTION

During previous studies, three sets of fuel designs for the HFIR core loaded with LEU U_3Si_3-Al dispersion fuel were proposed: 1) U_3Si_2-Al core [1], 2) high-density U_3Si_2-Al core [2], and 3) high-density U_3Si_2-Al with thick cladding [3]. These design efforts are part of the HFIR HEU to LEU to conversion activities funded by the Office of Material Management and Minimization (M3), National Nuclear Security Administration (NNSA), US Department of Energy (DOE). The HFIR conversion aims to design, qualify, fabricate, and deploy a HFIR LEU core that will maintain or exceed current reactor performance metrics and safety requirements at an affordable cost [4]. Specifically, the HFIR LEU core must demonstrate a maintained or enhanced ability to perform scientific missions, meet all the safety requirements, and minimize the annual operating cost. To achieve the same HEU core performance metrics and safety requirements, the core thermal power must be increased from 85 MW_{th} to 95 MW_{th} in the LEU designs.

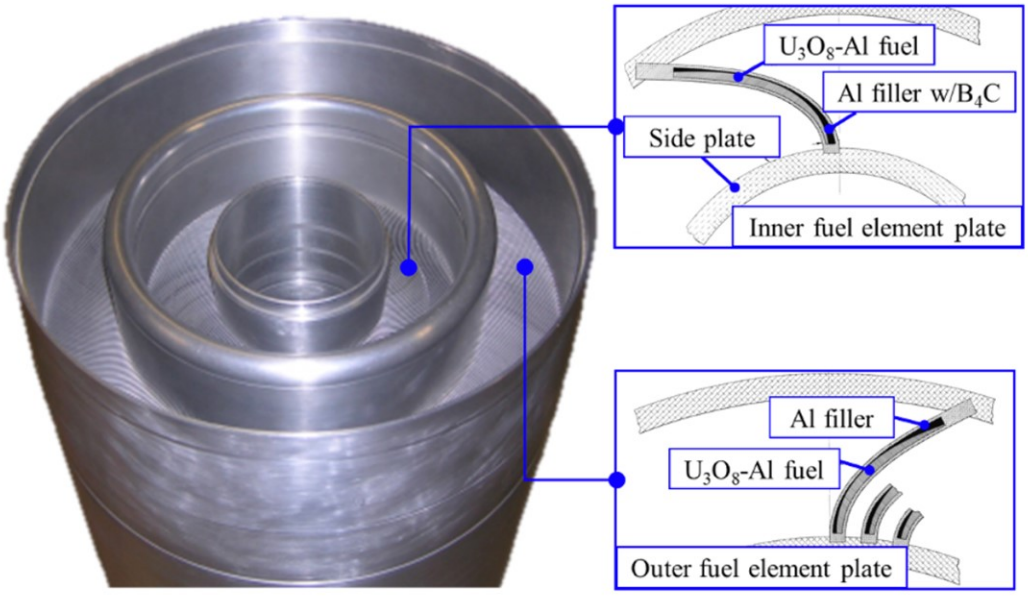

Figure 1. HFIR HEU fuel element.

In support of the HFIR LEU conversion efforts, this report quantifies the effect of uncertainty arising from the fuel inhomogeneity on the core performance metrics. *Fuel inhomogeneity* is defined as the deviation from the nominal distribution in the involute fuel plates resulting from manufacturing. The fabrication of the HFIR fuel plates is complex, not only due to the involute shape but also due to the variation of the fuel mixture along the arc of the involute. Initially, the fuel plate as shown in Fig. 1, including the fuel meat, filler, and cladding, is fabricated in a flat plate geometry, and then it is curved to obtain the involute shape. From the HEU fuel fabrication experience, the uranium inhomogeneity in a fuel plate is observed [5, 6, 7], and the fuel plate is rejected if the inhomogeneity detected by the scanner violates the +12% average or +27% local criteria [8]. Therefore, the tolerances are considered in the fuel specification, and uncertainty factors are applied in the safety analysis because the fuel inhomogeneity affects the reactor performance and safety.

The analysis of the fuel inhomogeneity uncertainty in the HFIR LEU core is important to determine the extent of HFIR LEU performance and safety sensitivity to the homogeneity distributions. However, the inhomogeneity distribution data from the fabrication of representative U_3Si_2-Al fuel plates are still lacking. Therefore, in this work, the fuel inhomogeneity profiles and tolerances were developed based on conservative

assumptions, HEU fuel fabrication and simulation experience, and the HEU U_3O_8-Al fuel specifications. Five inhomogeneity profiles were developed, including four conservative profiles described in Section 2. The considered inhomogeneity profiles are based on the +12% running average and streak requirements. Local spot violation of +27% is not considered. The analysis was performed with a low-density U_3Si_2-Al core at the beginning-of-cycle (BOC) with the control elements at their symmetrical critical position. Similar reactor performance changes due to fuel inhomogeneity profiles are expected for the other proposed HFIR LEU core designs. The impact of the fuel inhomogeneity uncertainty was evaluated using several key performance metrics such as multiplication factor (k_{eff}), cold source moderator vessel cold neutron flux and cold-to-total neutron flux ratio, ^{252}Cf target thermal neutron flux, flux trap fast neutron flux and fast-to-total neutron flux ratio, reflector fast neutron flux and fast-to-total neutron flux ratio, and fission rate density distribution [9]. The calculations were conducted using the massively parallel Monte Carlo radiation transport code Shift [10] developed at the ORNL in conjunction with ENDF/B-VII.0 nuclear data library [11].

2. INHOMOGENEITY PROFILES

Five inhomogeneity profiles were simulated to be used in this study. The inhomogeneity profile shows the ratio of the inhomogeneous uranium loading to the nominal uniform uranium loading in the fuel plates. The profiles were based on assumptions, experience with the HEU fuel, HEU fuel specifications, and loading scenarios resulting in additional fuel in thermally limiting regions. The profiles were translated into functions. Once the maximum local fuel inhomogeneity is determined, the inhomogeneity profile of a fuel plate is automatically provided. The profile matches the fuel region definition in the Shift input and it is applied to all fuel plates. The inner fuel element (IFE) plates are divided into 21 radial $\times$ 21 axial regions, and the outer fuel element (OFE) plates have 14 radial $\times$ 21 axial regions.

From the evaluation of all 369 OFE plates in Betzler et al.[5], it was observed that the fuel loading was larger than the nominal in the center region of the plate and peaked near the hump of the fuel region, whereas the fuel loading was less than nominal around the border of the fuel plates. The fuel distribution deviations from nominal were expected to be caused by the loading die. Considering this evaluation, the first profile, *peak hump 1*, was derived, as illustrated in Fig. 2 with a maximum local fuel inhomogeneity value of 12% at the fuel hump. The second profile, *peak hump 2*, is a conservative distribution of the first profile in which the inhomogeneity profile is observed only in the radial direction, as shown in Fig. 3, where the inhomogeneity values decrease as a function of nominal fuel thickness. Thus, these two distributions evaluate the impact of fuel overloading in the hump region of the fuel plates where the fuel thickness is greatest.

The three remaining profiles are also conservative inhomogeneity profiles developed to evaluate the impact of overloading the radial edges of the fuel plates where flux/power peaks typically occur because of their proximity to moderator and reflector regions. The *peak edge 1*, as depicted in Fig. 4, is the opposite of *peak hump 1*, in which the peak inhomogeneity is located at the thinnest fuel region. The peak +12% overloading occurs in the thinnest region of the fuel, the homogeneity values decrease with increased nominal fuel loading, and an axial profile is applied to maximize the fuel loading at the axial borders where flux/power peaks exist. In *peak edge 2*, the peak inhomogeneity is located at the top and bottom of both the innermost and outermost fuel region, as shown in Fig. 5. *Peak edges 1* and *2* are similar, but *peak edge 2* overloads both the inner and outer radial edges of the plate up to +12% and thus has a more underloaded hump region relative to *peak edge 1*. And the last profile, *peak edge 3*, has peak inhomogeneity along the fuel border of the fuel element, as illustrated in Fig. 6. All fuel distributions were derived so as to maintain nominal fuel plate uranium masses.

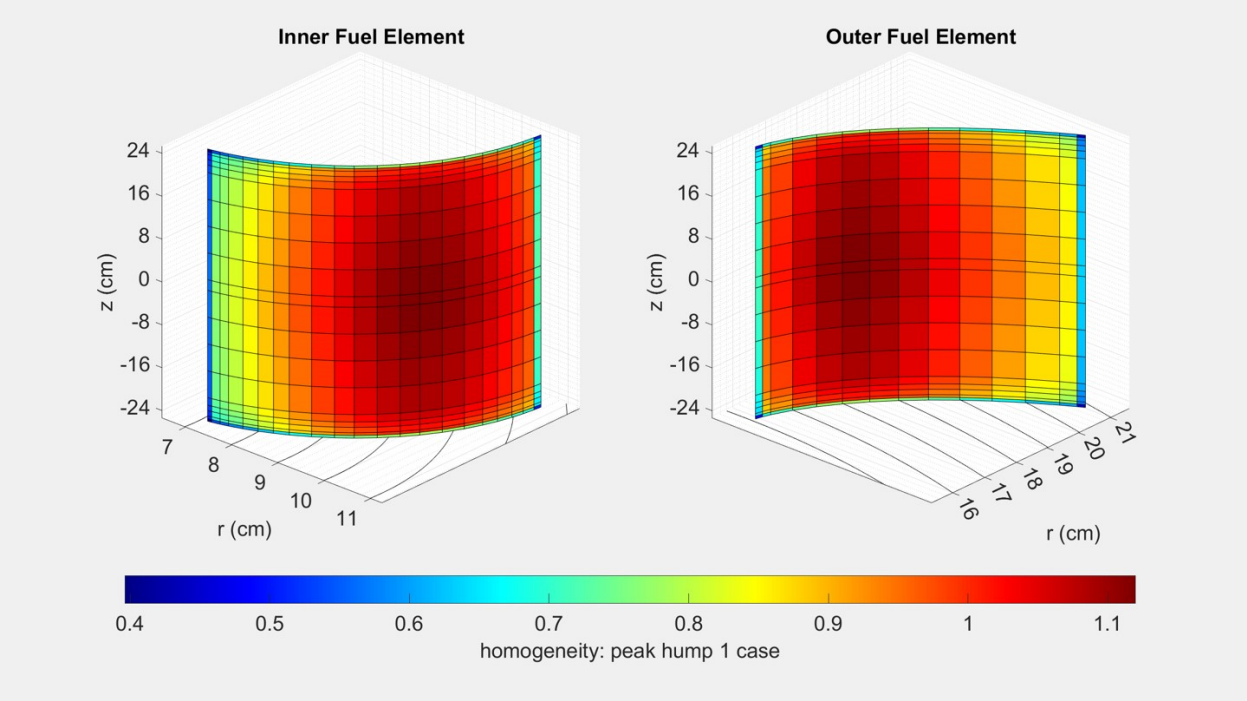

Figure 2. Inhomogeneity distribution of *peak hump 1* with maximum local fuel inhomogeneity of 1.12.

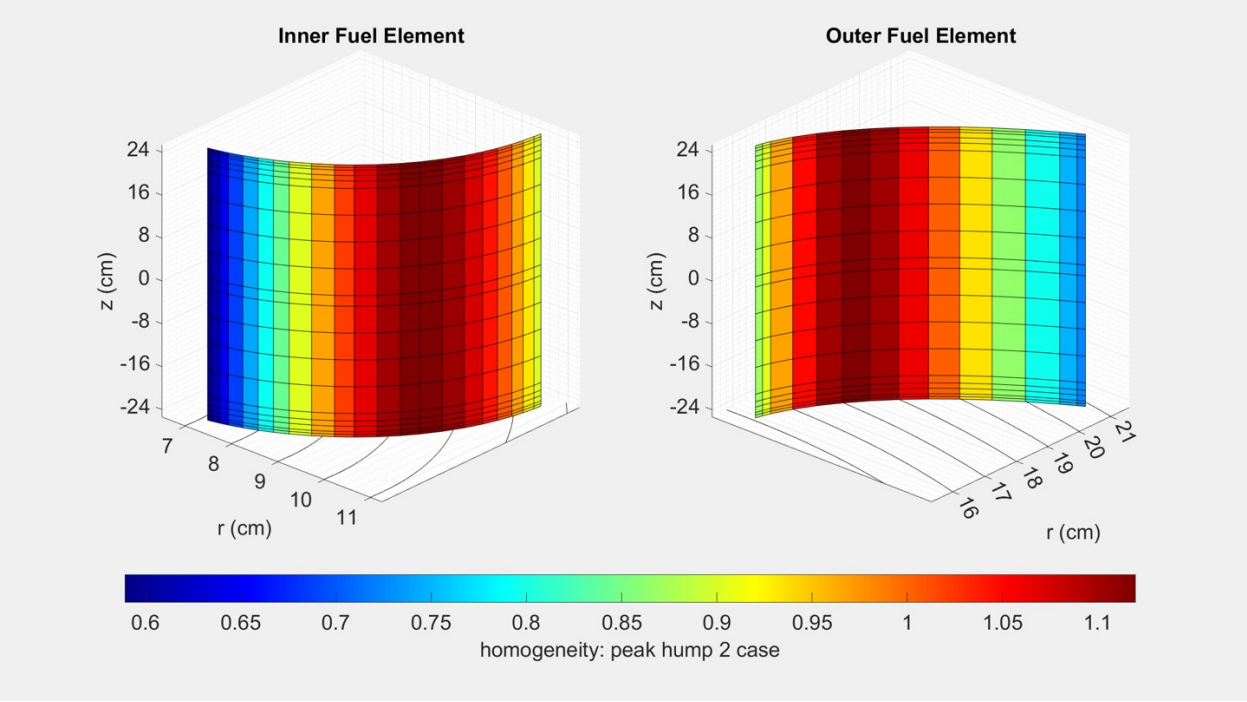

Figure 3. Inhomogeneity distribution of *peak hump 2* with maximum local fuel inhomogeneity of 1.12.

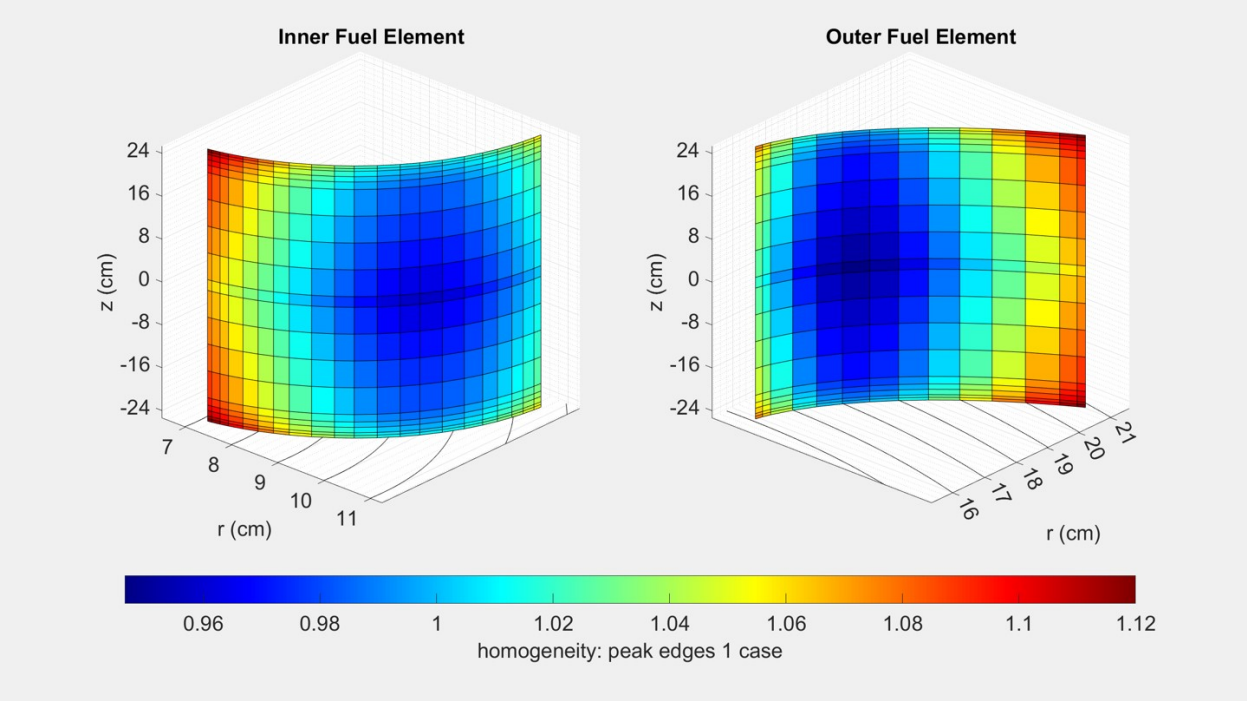

Figure 4. Inhomogeneity distribution of *peak edge 1* with maximum local fuel inhomogeneity of 1.12.

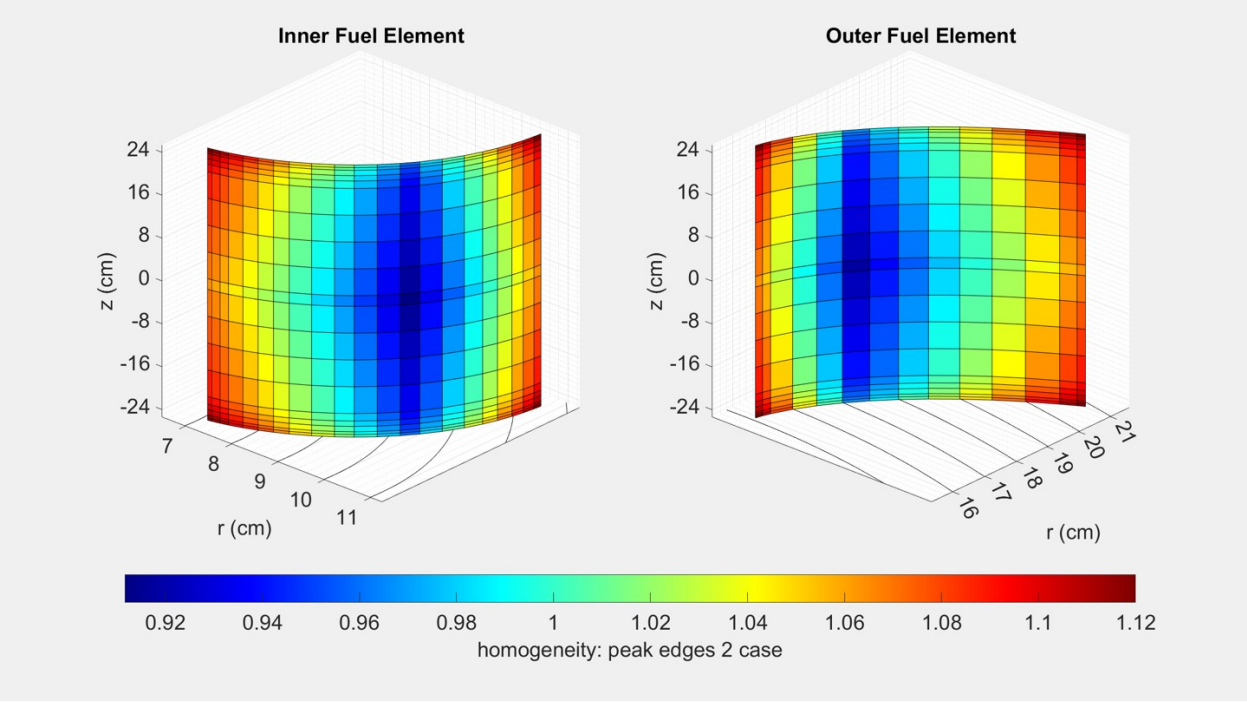

Figure 5. Inhomogeneity distribution of *peak edge 2* with maximum local fuel inhomogeneity of 1.12.

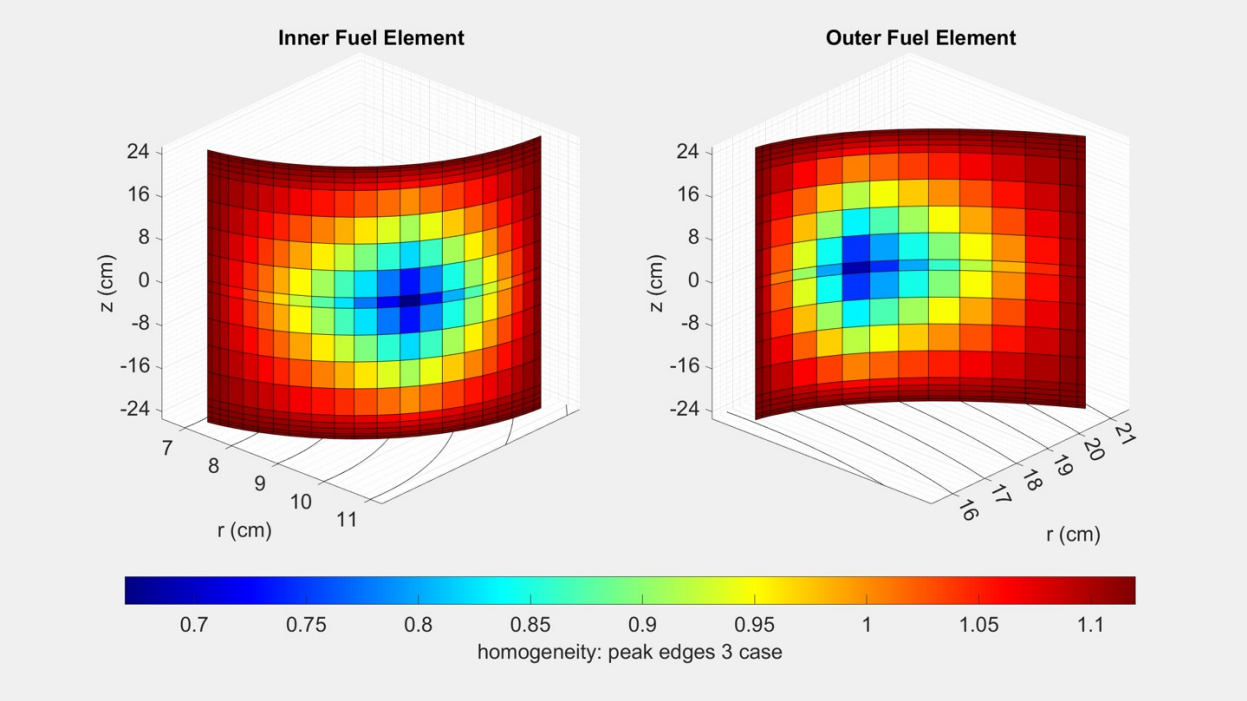

Figure 6. Inhomogeneity distribution of *peak edge 3* with maximum local fuel inhomogeneity of 1.12.

3. METHODOLOGY

3.1 CALCULATION METHODS

The continuous-energy Monte Carlo radiation transport code Shift [10] and ENDF/B-VII.0 [11] nuclear data library were used to calculate the reactor performance metrics. Six metrics are evaluated and discussed in the next section [9]. In Shift, the total number of neutrons per generation was 100,000, and the total cycles were 350 with 50 inactive cycles. The analyses were performed with the low-density U_3Si_2-Al optimized fuel design at BOC [1]; the control elements were at the critical positions calculated with the uniform fuel loading condition case. The uncertainty distributions listed in Table 1 were accounted for. The inhomogeneity profiles for the IFE and OFE were generated by considering the range of the local peak inhomogeneity values from 1.06 to 1.12 (0.01 stepping) on a normal distribution. The peak value of 1.06 was set as the minimum value because a value lower than this would produce a negligible inhomogeneity profile. The peak value of 1.12 was selected as the maximum because a fuel plate with an inhomogeneity value(s) exceeding +12% may be rejected or will be submitted for an explicit HFIR safety review to determine acceptability based on safety criteria guidelines. Later, each profile was used to perturb the density of the fuel cells in the IFE and OFE by multiplying the inhomogeneity value of each cell with its density. However, the volume of each fuel cell was kept the same as in the unperturbed case. An example of the inhomogeneity multiplier for each profile and peak factor of 1.06, 1.09, and 1.12 is available in Appendix A. The total samples generated were 246 input files representing the combinations of perturbations in the IFE and OFE for each inhomogeneity profile.

Table 1. Uncertainty parameters

Profile	Local peak inhomogeneity factor in IFE/OFE	Distribution
Peak hump 1	1.06 ~1.12	Uniform
Peak hump 2	1.06 ~1.12	Uniform
Peak edge 1	1.06 ~1.12	Uniform
Peak edge 2	1.06 ~1.12	Uniform
Peak edge 3	1.06 ~1.12	Uniform

3.2 PERFORMANCE METRICS

3.2.1 Multiplication Factor

Typically, the cycle length is used as one of the performance metrics for a HFIR core design. To obtain the cycle length, a depletion calculation is necessary. Since the depletion calculation is computationally expensive, it was not conducted in this work and will be considered in future studies. Instead, the multiplication factor k_{eff} at BOC was used as one of the metrics by evaluating the changes in k_{eff} value from the nominal case. The reduction in k_{eff} indirectly implies the reduction of cycle length and vice versa.

3.2.2 Cold Source Moderator Vessel Cold Flux and Ratio

The cold source flux magnitude and cold-to-total flux ratio are measures of the quality of the flux for cold neutron science. Increased brightness (i.e., greater magnitude) and reduced noise (i.e., higher cold-to-total flux ratio) are desired. Because the cold neutron source is radially external to the control elements, the cold source flux is highly affected by the control element location.

3.2.3 Curium/Californium Target Thermal Flux

Another important parameter to be evaluated is the ^{252}Cf production rate. Californium-252 is produced in HFIR by irradiating the curium oxide targets inside the flux trap region. To obtain the production rate, a depletion calculation is required. Since the depletion calculation was not performed in this work, the Cm target thermal flux was evaluated and compared to the nominal case. The reduction in the Cm target thermal flux implies the reduction of the ^{252}Cf production rate and vice versa.

3.2.4 Flux Trap Fast Flux and Ratio

The flux trap is the center region in HFIR that experiences the highest flux (about 10^{15} n $\cdot$ cm^{-2} $\cdot$ s^{-1}). The flux trap region is used for isotope production and materials irradiation testing. Fast flux in the flux trap is used for materials irradiation studies to accelerate damage testing. The fast flux and fast-to-total flux ratio metrics are calculated by spatially averaging the fast and non-fast fluxes in the material irradiation targets in the flux trap.

3.2.5 Reflector Fast Flux and Ratio

The removable beryllium reflector has eight large aluminum-lined irradiation positions, and one of these facilities is often used for materials irradiation purposes when large targets are irradiated. These metrics are calculated by spatially averaging the fluxes in the eight irradiation facilities (1A, 1B, 3A, 3B, 5A, 5B, 7A, and 7B) within the removable beryllium reflector region.

3.2.6 Fission Rate Density

The fission rate density f_d in a given fuel region in the unit of fissions per second per cm^3 of fuel particle is defined as

$$f_d = \frac{1}{V_{fuel}} \sum_i^M \int_0^\infty dE \int_{\partial V \in V_{fuel}} dV N_i(\mathbf{r}) \sigma_{i,f}(\mathbf{r}, E) \phi(\mathbf{r}, E) \tag{1}$$

where V_{fuel} is the volume of the given fuel region, N_i is the number density of isotope i, $\sigma_{i,f}$ is the fission cross section of isotope i, ϕ is the scalar flux, and the sum is over the M fissionable isotopes within the fuel region.

4. RESULTS AND DISCUSSION

4.1 IMPACT OF FUEL INHOMOGENEITY ON LEU CORE

The results from all perturbed cases are averaged and presented as a relative difference to the nominal (uniform fuel loading) case in Table 2. The inhomogeneity performance metrics except for the fission density are slightly decreased compared to the nominal case. However, the performance degradation is considered minor, with a relative difference of less than 0.5% with respect to that of the nominal case.

Table 2. Relative difference of the averaged evaluated performance metrics to the nominal case

Parameter	Relative difference
k_{eff}	-0.18 ±0.39
Cold source moderator vessel cold flux	-0.43 ±0.16
Cold source moderator vessel cold flux cold-to-fast flux ratio	-0.01 ±0.10
Thermal flux at Cm target	0.02 ±0.17
Flux trap fast flux	-0.28 ±0.10
Flux trap fast-to-total flux ratio	-0.25 ±0.20
Reflector fast flux	-0.18 ±0.10
Reflector fast-to-total flux ratio	-0.13 ±0.04

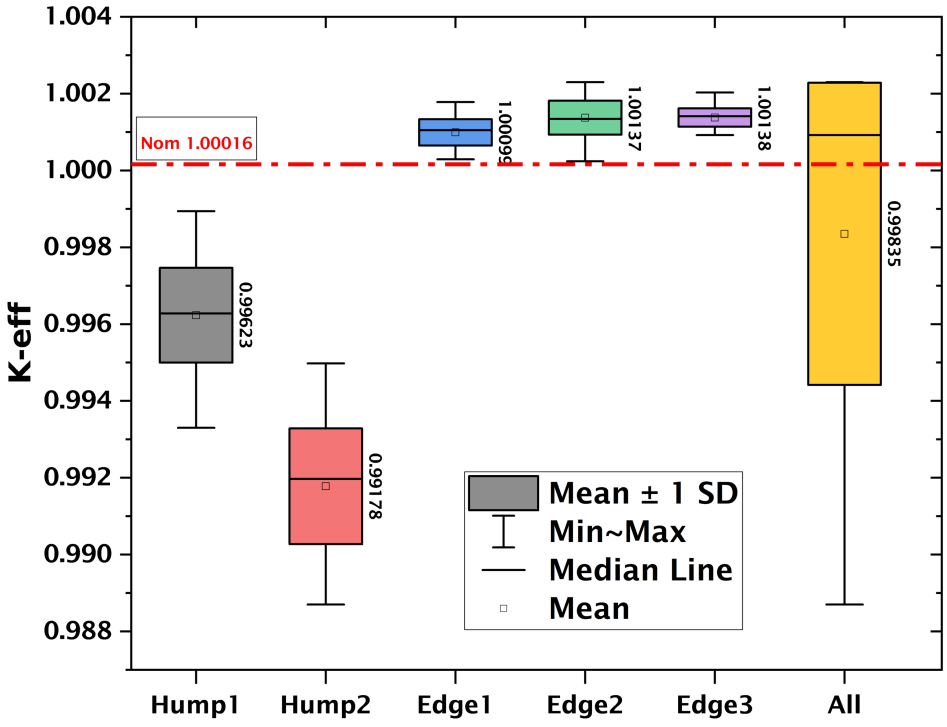

Figure 7. k_{eff} distribution of each profile and average (all).

The individual evaluation of each profile on the performance metrics also warrants discussion. The distribution of the k_{eff} at BOC for each inhomogeneity profile is shown in Figure 7. Both *hump* profiles result in the reduction of k_{eff} and, consequently, cycle length. For example, one of the cases in *hump 2* can reduce

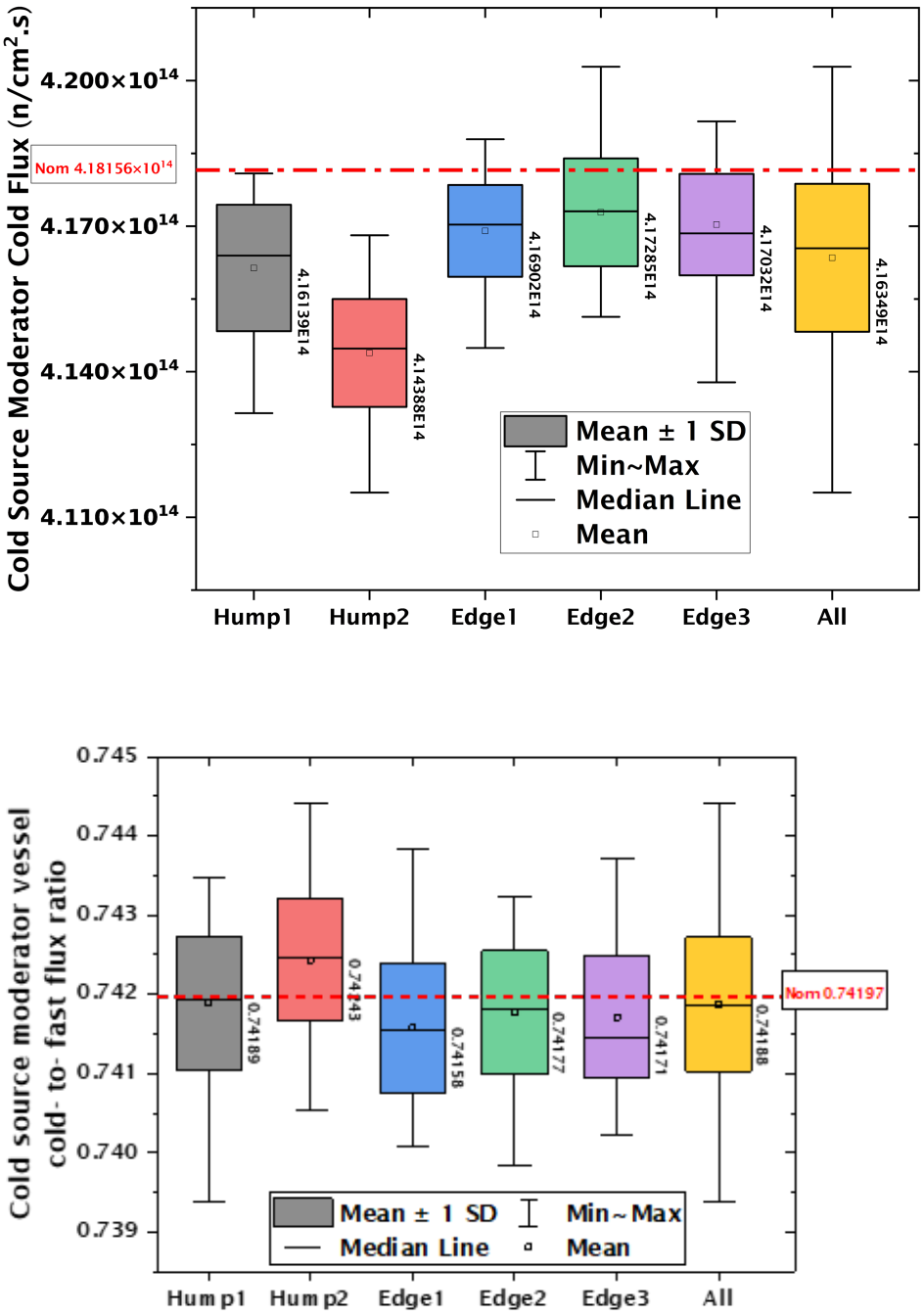

Figure 8. Cold source moderator cold flux and cold-to-fast flux ratio for each inhomogeneity profile and average (all).

the reactivity by about 1,158.9 ± 25.1 pcm. On the other hand, the *edge* profiles slightly increase k_{eff} since most of the fuels are distributed along the fuel plate frame next to the light water moderator. On average, the reduction of the multiplication factor is expected to be less than a day reduction in the cycle length (deduced

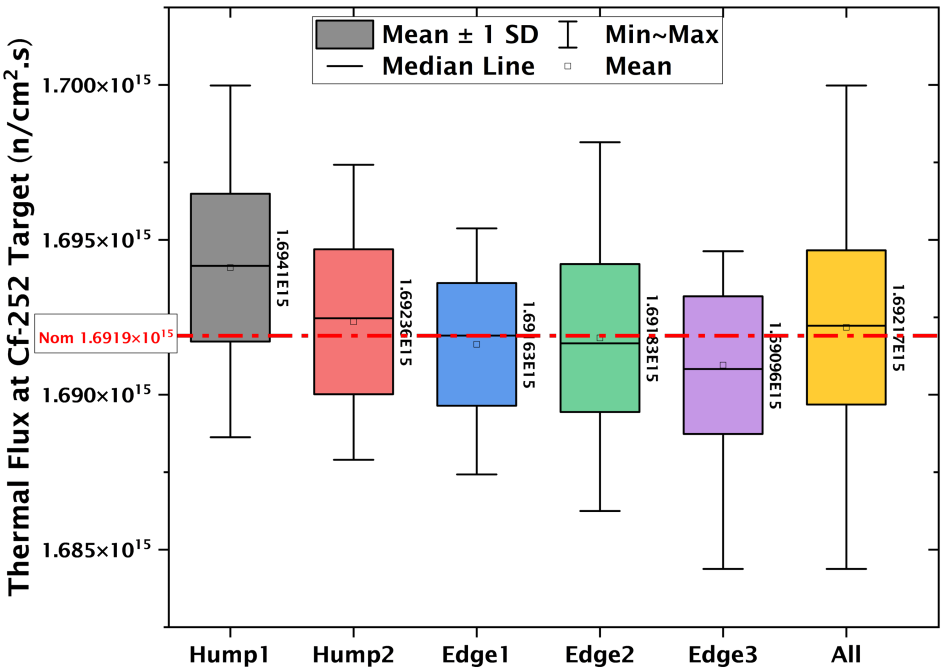

Figure 9. Thermal flux at Cm target for each inhomogeneity profile and average (all).

based on experience).

The performance metrics related to the thermal and fast fluxes at target locations are depicted in Figs. 8, 9, 10, and 11. Similar to the trend in the k_{eff}, profile *hump 2* shows a slight reduction in neutron fluxes compared to the other fuel inhomogeneity profiles. In profile *hump 2*, the uranium fuel is concentrated along the hump region. As a result, the fuel distribution in the periphery is significantly reduced, especially in the IFE inner radial edge next to the flux trap region and the OFE outer radial edge next to the beryllium reflector, contributing to the lower experiment regions' neutron flux in *hump 2*. Moreover, the neutron flux is also affected by the k_{eff} because it is used to obtain the absolute neutron flux in each target location. However, the change in average flux in each target due to the fuel inhomogeneity is considered negligible, with the relative difference ranging from -0.43% to 0.02%.

The relative difference of fission rate density compared with the nominal case caused by all inhomogeneity profiles for the IFE and OFE is shown in Fig. 12. The maximum average relative difference is about 3.22% and 3.74% in the IFE and OFE, respectively. On the other hand, the minimum relative difference in the IFE and OFE can be about -11.3% and -15.4%, respectively. As shown in Figs. 13 and 14, the fission rate density of each profile is dictated by the fuel inhomogeneity profile. For example, the reduction of the fission rate density at the plate periphery is up to 53% in the hump profiles. However, the maximum increase in a channel streak is about +7.58% and +9.19% for IFE and OFE, respectively, which is still lower than the uncertainty value considered in the steady-state thermal-hydraulics calculation, which is about +12%.

4.2 COMPARISON OF FUEL INHOMOGENEITY IN HFIR LEU AND HEU CORES

A similar assessment was also conducted by considering the fuel inhomogeneity in both the IFE and OFE for the HEU core. However, only the peak inhomogeneity factor of 1.12 was considered. Figure 15 shows that the trends in the performance metrics are similar between the HEU and LEU cores. Therefore, it is expected

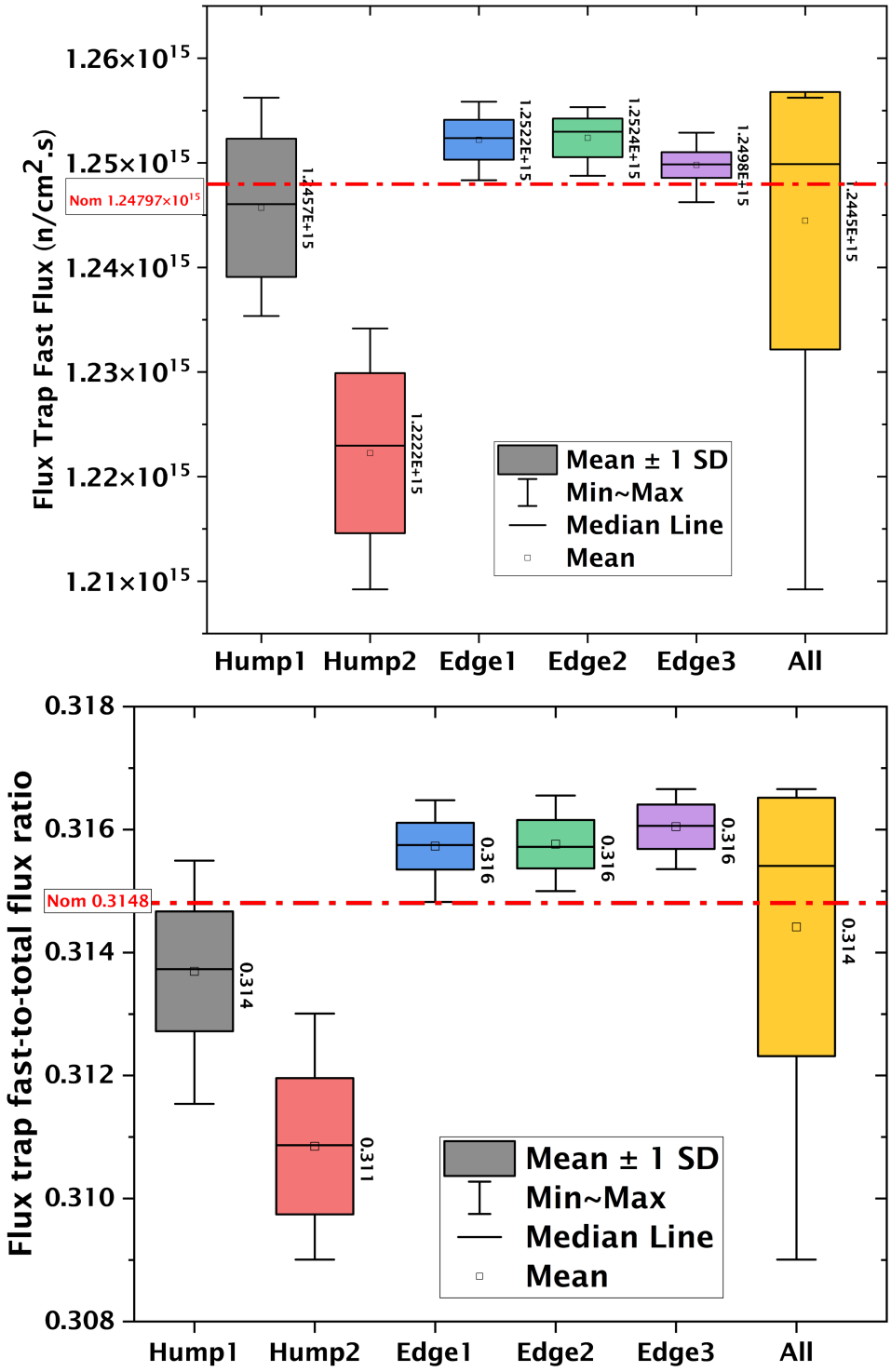

Figure 10. Flux trap flux and fast-to-total flux ratio for each inhomogeneity profile and average (all).

that the impact of the fuel inhomogeneity will be similar between the two cores, which is negligible with regard to reactor performance and bounded by safety analysis uncertainty factors with regard to fission rate densities.

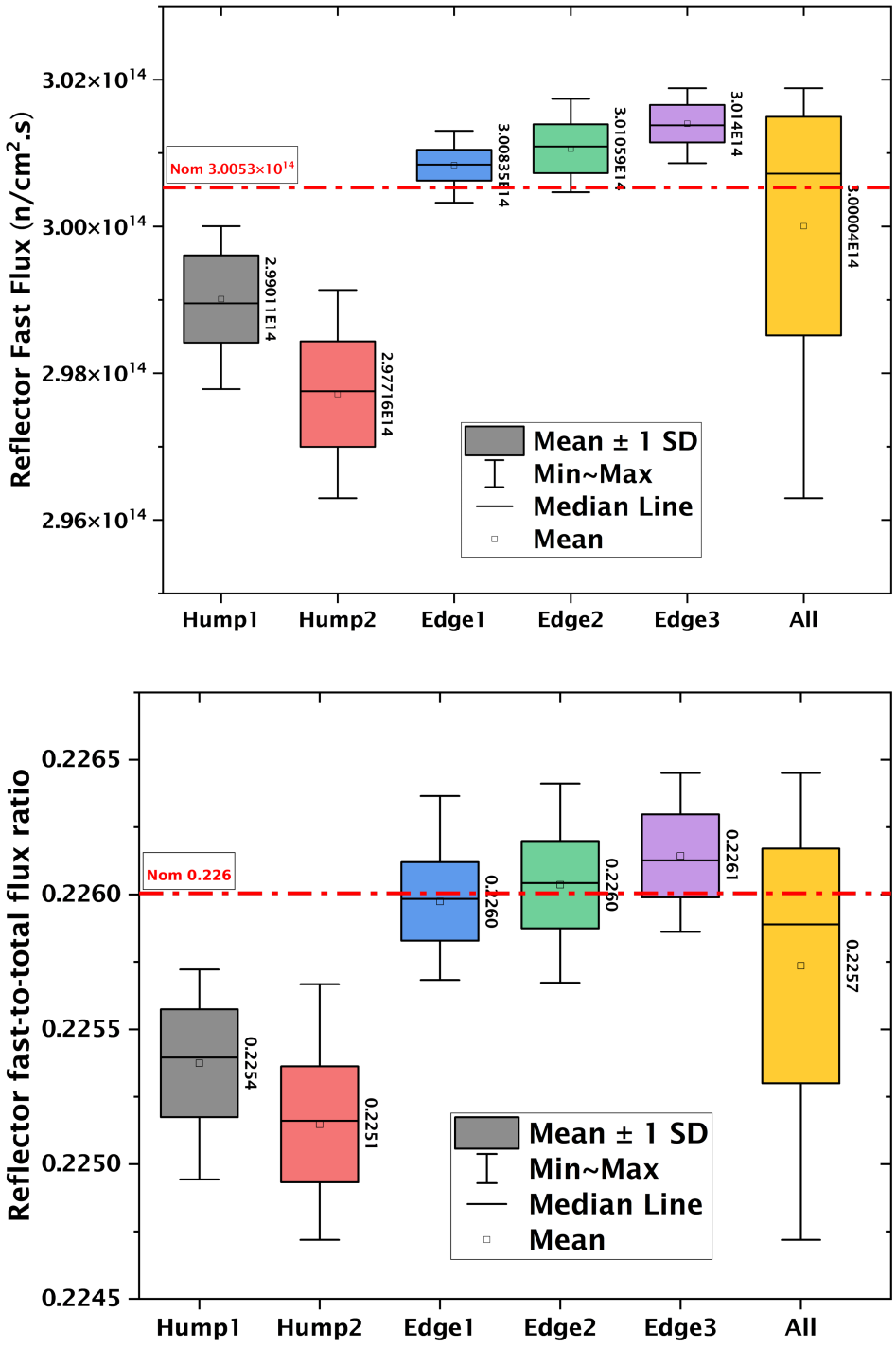

Figure 11. Reflector fast flux and fast-to-total flux ratio for each inhomogeneity profile and average (all).

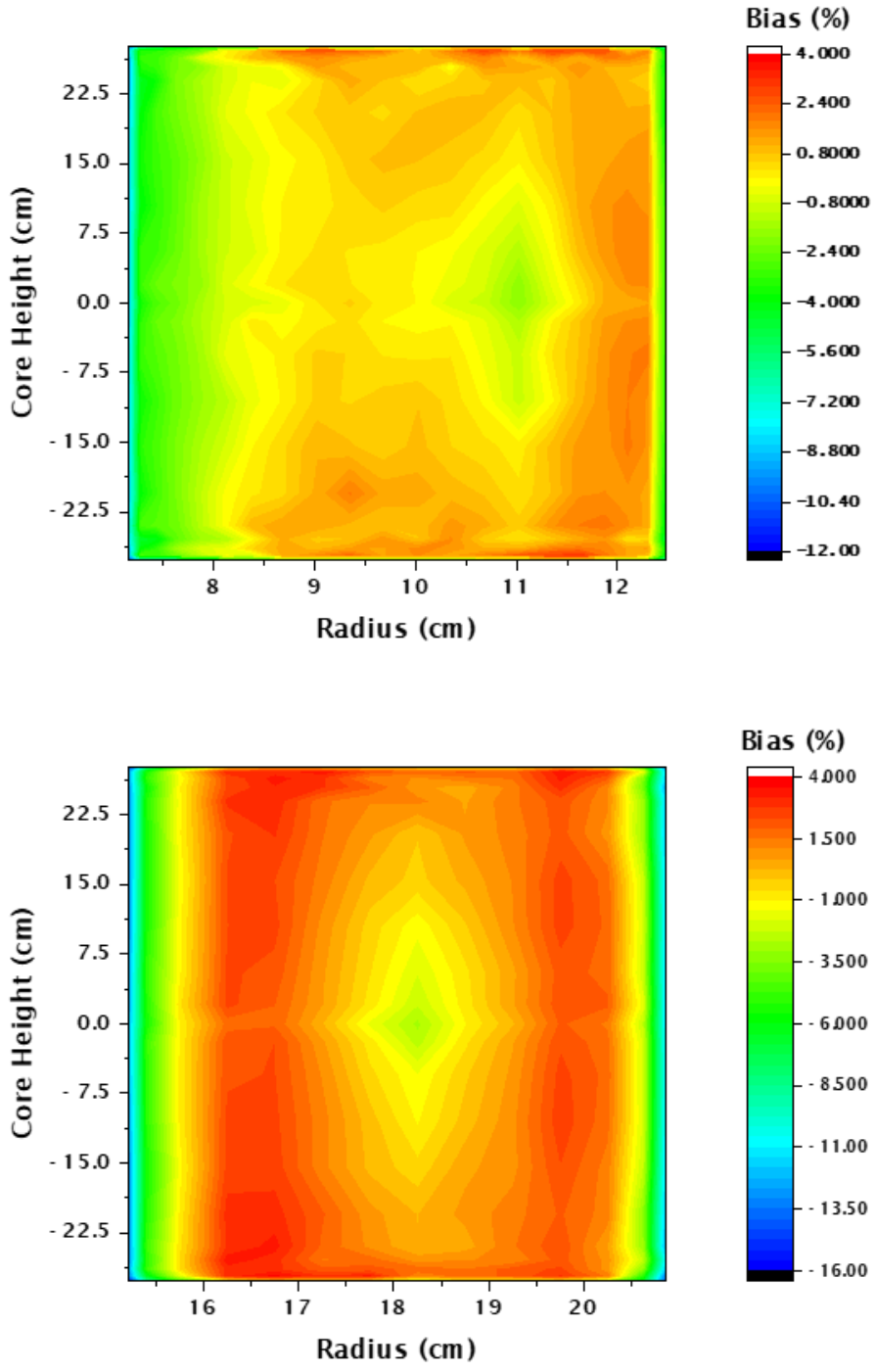

Figure 12. Fission rate density relative difference due to inhomogeneity to the nominal case in IFE (top) and OFE (bottom).

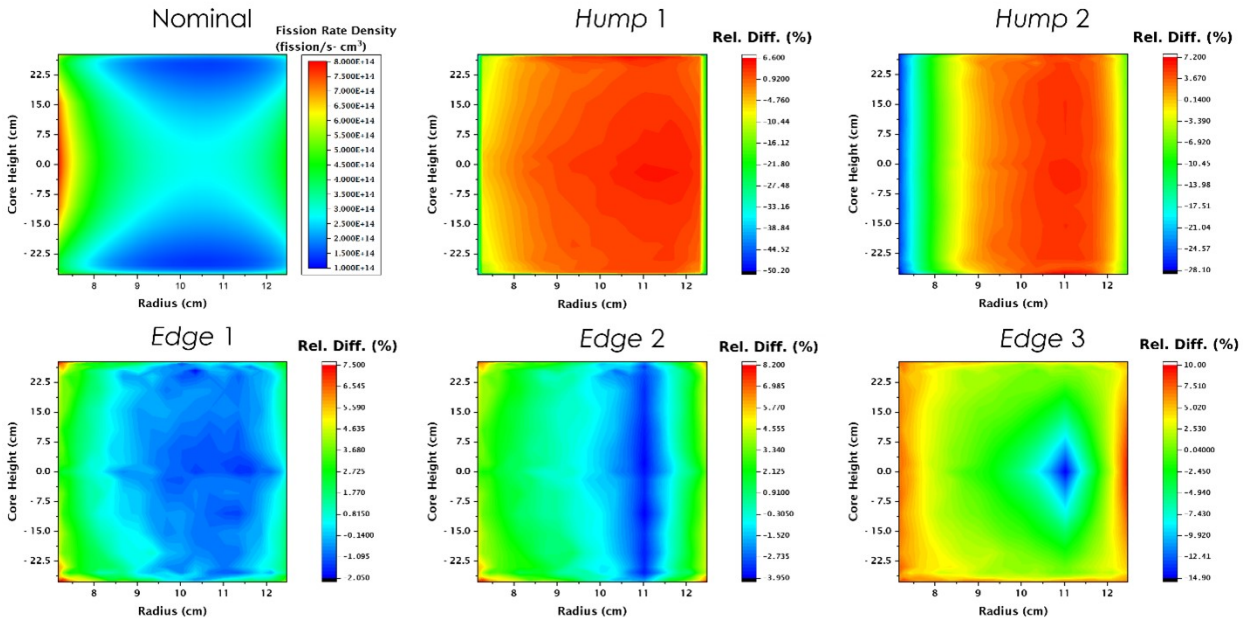

Figure 13. Fission rate density in IFE for nominal and its relative difference for each inhomogeneity profile. The volume in each fuel cell is the same between unperturbed and perturbed cases.

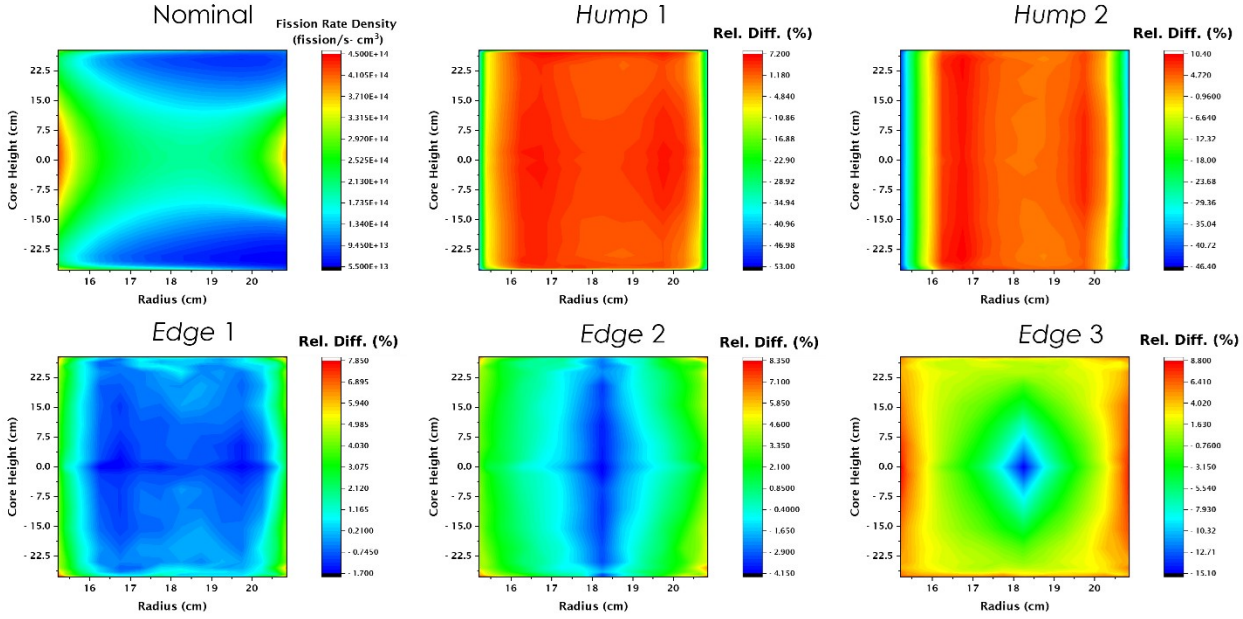

Figure 14. Fission rate density in OFE for nominal and its relative difference for each inhomogeneity profile. The volume in each fuel cell is the same between unperturbed and perturbed cases.

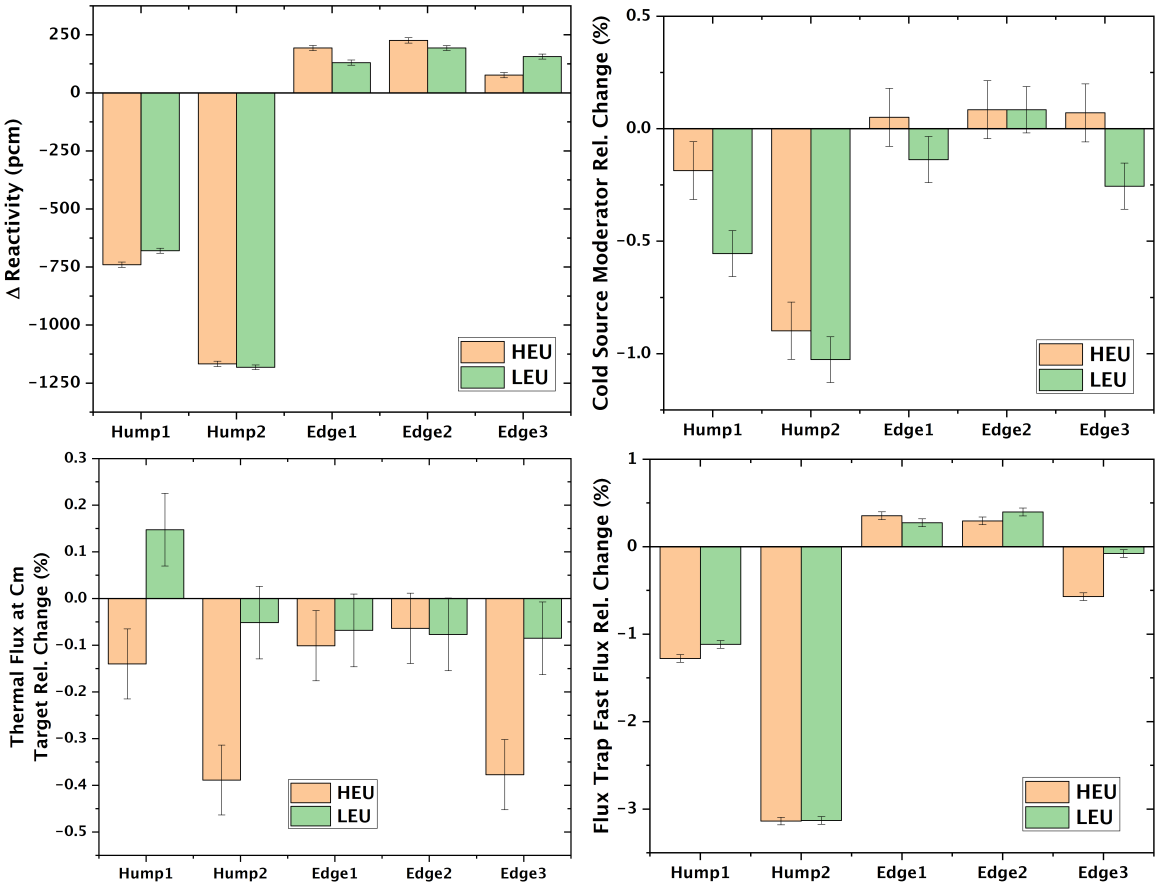

Figure 15. Comparison of several performance metrics between LEU and HEU cores due to fuel inhomogeneity.

5. CONCLUSIONS

The quantification of the uncertainty in the HFIR LEU core derived from the fuel inhomogeneity was carried out in this work. Five fuel inhomogeneity profiles were generated considering various assumptions, experience with the HEU fuel, HEU fuel specifications, and loading scenarios resulting in additional fuel in thermally limiting regions. The impact of fuel inhomogeneity on the key performance metrics was evaluated, and the impact in both HEU and LEU cores is similar. Performance metrics were on average reduced by less than 0.5% and can therefore be considered negligible. For future work, the uncertainty due to fuel inhomogeneity can also be quantified during the cycle (e.g., impact on cycle length, time-averaged fluxes). Moreover, other fuel-related uncertainty parameters — such as total fuel loading, uranium isotopic composition, coolant channel dimensions, and boron mass and impurities in the filler — can be carried out to complete the current study. The impact of the uncertainty parameters on the transient calculation can also be investigated.

REFERENCES

[1] B. R. Betzler, D. Chandler, J. Bae, G. Ilas, and M. J. L., "High Flux Isotope Reactor Low Enriched Uranium Low Density Silicide Fuel Design Parameters," Tech. Rep. ORNL/TM-2020/1798, Oak Ridge National Laboratory, March 2021.

[2] J. Bae, B. R. Betzler, D. Chandler, G. Ilas, and M. J. L., "High Flux Isotope Reactor Low-Enriched Uranium High Density Silicide Fuel Design Parameters," Tech. Rep. ORNL/TM-2020/1798, Oak Ridge National Laboratory, February 2021.

[3] J. Bae, B. R. Betzler, D. Chandler, G. Ilas, and M. J. L., "High Flux Isotope Reactor Low-Enriched Uranium High Density Silicide Thick Cladding Fuel Design Parameters," Tech. Rep. ORNL/TM-2021-1964, Oak Ridge National Laboratory, May 2021.

[4] R. T. Primm, III, R. J. Ellis, J. C. Gehin, D. L. Moses, J. L. Binder, and N. Xoubi, "Assumptions and Criteria for Performing a Feasability Study of the Conversion of the High Flux Isotope Reactor Core to Use Low-Enriched Uranium Fuel," Tech. Rep. ORNL/TM-2005/269, Oak Ridge National Laboratory, February 2006.

[5] B. R. Betzler, D. Chandler, T. M. Evans, G. G. Davidson, C. R. Daily, S. C. Wilson, and S. W. Mosher, "As-Built Simulation of the High Flux Isotope Reactor," *Journal of Nuclear Engineering*, vol. 2, no. 1, pp. 28–34, 2021.

[6] D. Chandler and C. J. Hurt, "As-Built Neutronic and Thermal Hydraulic Simulations of HFIR Outer Fuel Element O-475," Tech. Rep. ORNL/TM-2020/1809, Oak Ridge National Laboratory, September 2021.

[7] D. Chandler, "Evaluation of High Flux Isotope Reactor Pseudo Overloaded Inner Fuel Plates," Tech. Rep. ORNL/TM-2020/1825, Oak Ridge National Laboratory, January 2022.

[8] R. W. Knight and R. A. Morin, "Fabrication Procedures for Manufacturing High Flux Isotope Reactor Fuel Elements - II," Tech. Rep. ORNL/6852, Oak Ridge National Laboratory, December 1999.

[9] G. Ilas, B. R. Betzler, D. Chandler, D. G. Renfro, and E. E. Davidson, "Key metrics for HFIR HEU and LEU models," Tech. Rep. ORNL/TM-2016/581, Oak Ridge National Laboratory, October 2016.

[10] T. M. Pandya, S. R. Johnson, T. M. Evans, G. G. Davidson, S. P. Hamilton, and A. T. Godfrey, "Implementation, capabilities, and benchmarking of Shift, a massively parallel Monte Carlo radiation transport code," *Journal of Computational Physics*, vol. 308, pp. 239–272, 2016.

[11] M. Chadwick, P. Obložinský, M. Herman, N. Greene, R. McKnight, D. Smith, P. Young, R. MacFarlane, G. Hale, S. Frankle, A. Kahler, T. Kawano, R. Little, D. Madland, P. Moller, R. Mosteller, P. Page, P. Talou, H. Trellue, M. White, W. Wilson, R. Arcilla, C. Dunford, S. Mughabghab, B. Pritychenko, D. Rochman, A. Sonzogni, C. Lubitz, T. Trumbull, J. Weinman, D. Brown, D. Cullen, D. Heinrichs, D. McNabb, H. Derrien, M. Dunn, N. Larson, L. Leal, A. Carlson, R. Block, J. Briggs, E. Cheng, H. Huria, M. Zerkle, K. Kozier, A. Courcelle, V. Pronyaev, and S. van der Marck, "ENDF/B-VII.0: Next Generation Evaluated Nuclear Data Library for Nuclear Science and Technology," *Nuclear Data Sheets*, vol. 107, no. 12, pp. 2931–3060, 2006.

APPENDIX A. INHOMOGENEITY PROFILE MULTIPLIER

APPENDIX A. INHOMOGENEITY PROFILE MULTIPLIER

Inhomogeneity profile *hump 1* in IFE, local peak inhomogeneity factor of 1.12

	1	2	3	4	5	6	7	8	9	10	11	12	13	14	15	16	17	18	19	20	21
1	0.419	0.570	0.585	0.604	0.627	0.649	0.669	0.692	0.716	0.736	0.753	0.767	0.778	0.784	0.784	0.778	0.766	0.749	0.728	0.703	0.509
2	0.538	0.733	0.752	0.777	0.807	0.834	0.861	0.890	0.920	0.946	0.968	0.987	1.000	1.007	1.008	1.000	0.985	0.963	0.936	0.903	0.655
3	0.546	0.743	0.762	0.788	0.818	0.846	0.873	0.902	0.933	0.959	0.981	1.000	1.014	1.021	1.022	1.014	0.999	0.976	0.949	0.916	0.664
4	0.553	0.753	0.773	0.798	0.829	0.858	0.885	0.914	0.946	0.972	0.994	1.014	1.028	1.035	1.036	1.028	1.012	0.990	0.962	0.928	0.673
5	0.561	0.763	0.783	0.809	0.840	0.869	0.897	0.927	0.959	0.985	1.008	1.028	1.042	1.049	1.050	1.042	1.026	1.003	0.975	0.941	0.682
6	0.568	0.773	0.794	0.820	0.851	0.881	0.909	0.939	0.972	0.998	1.021	1.042	1.056	1.063	1.064	1.056	1.040	1.017	0.988	0.954	0.691
7	0.575	0.783	0.804	0.831	0.863	0.892	0.921	0.951	0.984	1.012	1.035	1.055	1.069	1.077	1.078	1.070	1.054	1.030	1.001	0.966	0.700
8	0.583	0.794	0.815	0.842	0.874	0.904	0.932	0.964	0.997	1.025	1.048	1.069	1.083	1.091	1.092	1.083	1.067	1.043	1.014	0.979	0.709
9	0.590	0.804	0.825	0.852	0.885	0.916	0.944	0.976	1.010	1.038	1.062	1.083	1.097	1.105	1.106	1.097	1.081	1.057	1.027	0.991	0.718
10	0.598	0.814	0.836	0.863	0.896	0.927	0.956	0.989	1.023	1.051	1.075	1.096	1.111	1.119	1.120	1.111	1.095	1.070	1.040	1.004	0.727
11	0.598	0.814	0.836	0.863	0.896	0.927	0.956	0.989	1.023	1.051	1.075	1.096	1.111	1.119	1.120	1.111	1.095	1.070	1.040	1.004	0.727
12	0.598	0.814	0.836	0.863	0.896	0.927	0.956	0.989	1.023	1.051	1.075	1.096	1.111	1.119	1.120	1.111	1.095	1.070	1.040	1.004	0.727
13	0.590	0.804	0.825	0.852	0.885	0.916	0.944	0.976	1.010	1.038	1.062	1.083	1.097	1.105	1.106	1.097	1.081	1.057	1.027	0.991	0.718
14	0.583	0.794	0.815	0.842	0.874	0.904	0.932	0.964	0.997	1.025	1.048	1.069	1.083	1.091	1.092	1.083	1.067	1.043	1.014	0.979	0.709
15	0.575	0.783	0.804	0.831	0.863	0.892	0.921	0.951	0.984	1.012	1.035	1.055	1.069	1.077	1.078	1.070	1.054	1.030	1.001	0.966	0.700
16	0.568	0.773	0.794	0.820	0.851	0.881	0.909	0.939	0.972	0.998	1.021	1.042	1.056	1.063	1.064	1.056	1.040	1.017	0.988	0.954	0.691
17	0.561	0.763	0.783	0.809	0.840	0.869	0.897	0.927	0.959	0.985	1.008	1.028	1.042	1.049	1.050	1.042	1.026	1.003	0.975	0.941	0.682
18	0.553	0.753	0.773	0.798	0.829	0.858	0.885	0.914	0.946	0.972	0.994	1.014	1.028	1.035	1.036	1.028	1.012	0.990	0.962	0.928	0.673
19	0.546	0.743	0.762	0.788	0.818	0.846	0.873	0.902	0.933	0.959	0.981	1.000	1.014	1.021	1.022	1.014	0.999	0.976	0.949	0.916	0.664
20	0.538	0.733	0.752	0.777	0.807	0.834	0.861	0.890	0.920	0.946	0.968	0.987	1.000	1.007	1.008	1.000	0.985	0.963	0.936	0.903	0.655
21	0.419	0.570	0.585	0.604	0.627	0.649	0.669	0.692	0.716	0.736	0.753	0.767	0.778	0.784	0.784	0.778	0.766	0.749	0.728	0.703	0.509

Inhomogeneity profile *hump 1* in OFE, local peak inhomogeneity factor of 1.12

	1	2	3	4	5	6	7	8	9	10	11	12	13	14
1	0.341	0.520	0.624	0.739	0.784	0.784	0.784	0.784	0.784	0.784	0.784	0.720	0.603	0.372
2	0.439	0.669	0.803	0.950	1.008	1.008	1.008	1.008	1.008	1.008	1.008	0.926	0.776	0.478
3	0.445	0.678	0.814	0.964	1.022	1.022	1.022	1.022	1.022	1.022	1.022	0.939	0.787	0.485
4	0.451	0.687	0.825	0.977	1.036	1.036	1.036	1.036	1.036	1.036	1.036	0.952	0.797	0.491
5	0.457	0.697	0.836	0.990	1.050	1.050	1.050	1.050	1.050	1.050	1.050	0.965	0.808	0.498
6	0.463	0.706	0.847	1.003	1.064	1.064	1.064	1.064	1.064	1.064	1.064	0.977	0.819	0.504
7	0.469	0.715	0.859	1.016	1.078	1.078	1.078	1.078	1.078	1.078	1.078	0.990	0.830	0.511
8	0.475	0.724	0.870	1.030	1.092	1.092	1.092	1.092	1.092	1.092	1.092	1.003	0.840	0.518
9	0.482	0.734	0.881	1.043	1.106	1.106	1.106	1.106	1.106	1.106	1.106	1.016	0.851	0.524
10	0.488	0.743	0.892	1.056	1.120	1.120	1.120	1.120	1.120	1.120	1.120	1.029	0.862	0.531
11	0.488	0.743	0.892	1.056	1.120	1.120	1.120	1.120	1.120	1.120	1.120	1.029	0.862	0.531
12	0.488	0.743	0.892	1.056	1.120	1.120	1.120	1.120	1.120	1.120	1.120	1.029	0.862	0.531
13	0.482	0.734	0.881	1.043	1.106	1.106	1.106	1.106	1.106	1.106	1.106	1.016	0.851	0.524
14	0.475	0.724	0.870	1.030	1.092	1.092	1.092	1.092	1.092	1.092	1.092	1.003	0.840	0.518
15	0.469	0.715	0.859	1.016	1.078	1.078	1.078	1.078	1.078	1.078	1.078	0.990	0.830	0.511
16	0.463	0.706	0.847	1.003	1.064	1.064	1.064	1.064	1.064	1.064	1.064	0.977	0.819	0.504
17	0.457	0.697	0.836	0.990	1.050	1.050	1.050	1.050	1.050	1.050	1.050	0.965	0.808	0.498
18	0.451	0.687	0.825	0.977	1.036	1.036	1.036	1.036	1.036	1.036	1.036	0.952	0.797	0.491
19	0.445	0.678	0.814	0.964	1.022	1.022	1.022	1.022	1.022	1.022	1.022	0.939	0.787	0.485
20	0.439	0.669	0.803	0.950	1.008	1.008	1.008	1.008	1.008	1.008	1.008	0.926	0.776	0.478
21	0.341	0.520	0.624	0.739	0.784	0.784	0.784	0.784	0.784	0.784	0.784	0.720	0.603	0.372

Inhomogeneity profile *hump 1* in IFE, local peak inhomogeneity factor of 1.09

	1	2	3	4	5	6	7	8	9	10	11	12	13	14	15	16	17	18	19	20	21
1	0.474	0.639	0.647	0.659	0.672	0.685	0.697	0.710	0.723	0.735	0.745	0.753	0.759	0.763	0.763	0.759	0.753	0.743	0.730	0.716	0.527
2	0.609	0.821	0.832	0.847	0.864	0.880	0.896	0.912	0.930	0.945	0.958	0.969	0.976	0.981	0.981	0.976	0.968	0.955	0.939	0.920	0.678
3	0.618	0.833	0.844	0.859	0.876	0.893	0.908	0.925	0.943	0.958	0.971	0.982	0.990	0.994	0.995	0.990	0.981	0.968	0.952	0.933	0.688
4	0.626	0.844	0.856	0.870	0.888	0.905	0.920	0.938	0.956	0.971	0.984	0.996	1.003	1.008	1.008	1.004	0.995	0.981	0.965	0.946	0.697
5	0.635	0.855	0.867	0.882	0.900	0.917	0.933	0.950	0.969	0.984	0.997	1.009	1.017	1.022	1.022	1.017	1.008	0.995	0.978	0.959	0.706
6	0.643	0.867	0.879	0.894	0.912	0.929	0.945	0.963	0.982	0.997	1.011	1.022	1.031	1.035	1.036	1.031	1.021	1.008	0.991	0.971	0.716
7	0.652	0.878	0.890	0.906	0.924	0.941	0.958	0.976	0.995	1.011	1.024	1.036	1.044	1.049	1.049	1.044	1.035	1.021	1.004	0.984	0.725
8	0.660	0.890	0.902	0.917	0.936	0.954	0.970	0.988	1.008	1.024	1.037	1.049	1.058	1.062	1.063	1.058	1.048	1.034	1.017	0.997	0.735
9	0.669	0.901	0.913	0.929	0.948	0.966	0.983	1.001	1.021	1.037	1.051	1.063	1.071	1.076	1.076	1.071	1.062	1.048	1.030	1.010	0.744
10	0.677	0.912	0.925	0.941	0.960	0.978	0.995	1.014	1.034	1.050	1.064	1.076	1.085	1.090	1.090	1.085	1.075	1.061	1.043	1.023	0.753
11	0.677	0.912	0.925	0.941	0.960	0.978	0.995	1.014	1.034	1.050	1.064	1.076	1.085	1.090	1.090	1.085	1.075	1.061	1.043	1.023	0.753
12	0.677	0.912	0.925	0.941	0.960	0.978	0.995	1.014	1.034	1.050	1.064	1.076	1.085	1.090	1.090	1.085	1.075	1.061	1.043	1.023	0.753
13	0.669	0.901	0.913	0.929	0.948	0.966	0.983	1.001	1.021	1.037	1.051	1.063	1.071	1.076	1.076	1.071	1.062	1.048	1.030	1.010	0.744
14	0.660	0.890	0.902	0.917	0.936	0.954	0.970	0.988	1.008	1.024	1.037	1.049	1.058	1.062	1.063	1.058	1.048	1.034	1.017	0.997	0.735
15	0.652	0.878	0.890	0.906	0.924	0.941	0.958	0.976	0.995	1.011	1.024	1.036	1.044	1.049	1.049	1.044	1.035	1.021	1.004	0.984	0.725
16	0.643	0.867	0.879	0.894	0.912	0.929	0.945	0.963	0.982	0.997	1.011	1.022	1.031	1.035	1.036	1.031	1.021	1.008	0.991	0.971	0.716
17	0.635	0.855	0.867	0.882	0.900	0.917	0.933	0.950	0.969	0.984	0.997	1.009	1.017	1.022	1.022	1.017	1.008	0.995	0.978	0.959	0.706
18	0.626	0.844	0.856	0.870	0.888	0.905	0.920	0.938	0.956	0.971	0.984	0.996	1.003	1.008	1.008	1.004	0.995	0.981	0.965	0.946	0.697
19	0.618	0.833	0.844	0.859	0.876	0.893	0.908	0.925	0.943	0.958	0.971	0.982	0.990	0.994	0.995	0.990	0.981	0.968	0.952	0.933	0.688
20	0.609	0.821	0.832	0.847	0.864	0.880	0.896	0.912	0.930	0.945	0.958	0.969	0.976	0.981	0.981	0.976	0.968	0.955	0.939	0.920	0.678
21	0.474	0.639	0.647	0.659	0.672	0.685	0.697	0.710	0.723	0.735	0.745	0.753	0.759	0.763	0.763	0.759	0.753	0.743	0.730	0.716	0.527

Inhomogeneity profile *hump 1* in OFE, local peak inhomogeneity factor of 1.09

	1	2	3	4	5	6	7	8	9	10	11	12	13	14
1	0.436	0.617	0.675	0.738	0.763	0.763	0.763	0.763	0.763	0.763	0.763	0.728	0.663	0.452
2	0.560	0.793	0.867	0.949	0.981	0.981	0.981	0.981	0.981	0.981	0.981	0.936	0.852	0.582
3	0.568	0.804	0.879	0.962	0.995	0.995	0.995	0.995	0.995	0.995	0.995	0.949	0.864	0.590
4	0.576	0.815	0.891	0.975	1.008	1.008	1.008	1.008	1.008	1.008	1.008	0.962	0.876	0.598
5	0.583	0.826	0.903	0.989	1.022	1.022	1.022	1.022	1.022	1.022	1.022	0.975	0.888	0.606
6	0.591	0.837	0.915	1.002	1.036	1.036	1.036	1.036	1.036	1.036	1.036	0.988	0.900	0.614
7	0.599	0.848	0.928	1.015	1.049	1.049	1.049	1.049	1.049	1.049	1.049	1.001	0.911	0.622
8	0.607	0.859	0.940	1.028	1.063	1.063	1.063	1.063	1.063	1.063	1.063	1.014	0.923	0.630
9	0.614	0.870	0.952	1.041	1.076	1.076	1.076	1.076	1.076	1.076	1.076	1.027	0.935	0.638
10	0.622	0.881	0.964	1.054	1.090	1.090	1.090	1.090	1.090	1.090	1.090	1.040	0.947	0.646
11	0.622	0.881	0.964	1.054	1.090	1.090	1.090	1.090	1.090	1.090	1.090	1.040	0.947	0.646
12	0.622	0.881	0.964	1.054	1.090	1.090	1.090	1.090	1.090	1.090	1.090	1.040	0.947	0.646
13	0.614	0.870	0.952	1.041	1.076	1.076	1.076	1.076	1.076	1.076	1.076	1.027	0.935	0.638
14	0.607	0.859	0.940	1.028	1.063	1.063	1.063	1.063	1.063	1.063	1.063	1.014	0.923	0.630
15	0.599	0.848	0.928	1.015	1.049	1.049	1.049	1.049	1.049	1.049	1.049	1.001	0.911	0.622
16	0.591	0.837	0.915	1.002	1.036	1.036	1.036	1.036	1.036	1.036	1.036	0.988	0.900	0.614
17	0.583	0.826	0.903	0.989	1.022	1.022	1.022	1.022	1.022	1.022	1.022	0.975	0.888	0.606
18	0.576	0.815	0.891	0.975	1.008	1.008	1.008	1.008	1.008	1.008	1.008	0.962	0.876	0.598
19	0.568	0.804	0.879	0.962	0.995	0.995	0.995	0.995	0.995	0.995	0.995	0.949	0.864	0.590
20	0.560	0.793	0.867	0.949	0.981	0.981	0.981	0.981	0.981	0.981	0.981	0.936	0.852	0.582
21	0.436	0.617	0.675	0.738	0.763	0.763	0.763	0.763	0.763	0.763	0.763	0.728	0.663	0.452

Inhomogeneity profile *hump 1* in IFE, local peak inhomogeneity factor of 1.06

	1	2	3	4	5	6	7	8	9	10	11	12	13	14	15	16	17	18	19	20	21
1	0.529	0.708	0.710	0.713	0.717	0.720	0.724	0.727	0.731	0.734	0.737	0.739	0.741	0.742	0.742	0.741	0.739	0.736	0.733	0.729	0.546
2	0.680	0.910	0.913	0.917	0.922	0.926	0.930	0.935	0.940	0.944	0.948	0.951	0.953	0.954	0.954	0.953	0.950	0.947	0.942	0.937	0.702
3	0.690	0.922	0.926	0.930	0.934	0.939	0.943	0.948	0.953	0.957	0.961	0.964	0.966	0.967	0.967	0.966	0.964	0.960	0.955	0.950	0.711
4	0.699	0.935	0.938	0.942	0.947	0.952	0.956	0.961	0.966	0.970	0.974	0.977	0.979	0.980	0.981	0.979	0.977	0.973	0.969	0.963	0.721
5	0.709	0.948	0.951	0.955	0.960	0.965	0.969	0.974	0.979	0.983	0.987	0.990	0.992	0.994	0.994	0.992	0.990	0.986	0.982	0.976	0.731
6	0.718	0.960	0.964	0.968	0.973	0.978	0.982	0.987	0.992	0.996	1.000	1.003	1.006	1.007	1.007	1.006	1.003	0.999	0.995	0.989	0.741
7	0.728	0.973	0.976	0.981	0.986	0.990	0.995	1.000	1.005	1.010	1.013	1.017	1.019	1.020	1.020	1.019	1.016	1.013	1.008	1.002	0.750
8	0.737	0.986	0.989	0.993	0.998	1.003	1.008	1.013	1.018	1.023	1.026	1.030	1.032	1.033	1.034	1.032	1.030	1.026	1.021	1.015	0.760
9	0.747	0.998	1.002	1.006	1.011	1.016	1.021	1.026	1.031	1.036	1.040	1.043	1.045	1.047	1.047	1.045	1.043	1.039	1.034	1.028	0.770
10	0.756	1.011	1.014	1.019	1.024	1.029	1.034	1.039	1.044	1.049	1.053	1.056	1.059	1.060	1.060	1.059	1.056	1.052	1.047	1.041	0.780
11	0.756	1.011	1.014	1.019	1.024	1.029	1.034	1.039	1.044	1.049	1.053	1.056	1.059	1.060	1.060	1.059	1.056	1.052	1.047	1.041	0.780
12	0.756	1.011	1.014	1.019	1.024	1.029	1.034	1.039	1.044	1.049	1.053	1.056	1.059	1.060	1.060	1.059	1.056	1.052	1.047	1.041	0.780
13	0.747	0.998	1.002	1.006	1.011	1.016	1.021	1.026	1.031	1.036	1.040	1.043	1.045	1.047	1.047	1.045	1.043	1.039	1.034	1.028	0.770
14	0.737	0.986	0.989	0.993	0.998	1.003	1.008	1.013	1.018	1.023	1.026	1.030	1.032	1.033	1.034	1.032	1.030	1.026	1.021	1.015	0.760
15	0.728	0.973	0.976	0.981	0.986	0.990	0.995	1.000	1.005	1.010	1.013	1.017	1.019	1.020	1.020	1.019	1.016	1.013	1.008	1.002	0.750
16	0.718	0.960	0.964	0.968	0.973	0.978	0.982	0.987	0.992	0.996	1.000	1.003	1.006	1.007	1.007	1.006	1.003	0.999	0.995	0.989	0.741
17	0.709	0.948	0.951	0.955	0.960	0.965	0.969	0.974	0.979	0.983	0.987	0.990	0.992	0.994	0.994	0.992	0.990	0.986	0.982	0.976	0.731
18	0.699	0.935	0.938	0.942	0.947	0.952	0.956	0.961	0.966	0.970	0.974	0.977	0.979	0.980	0.981	0.979	0.977	0.973	0.969	0.963	0.721
19	0.690	0.922	0.926	0.930	0.934	0.939	0.943	0.948	0.953	0.957	0.961	0.964	0.966	0.967	0.967	0.966	0.964	0.960	0.955	0.950	0.711
20	0.680	0.910	0.913	0.917	0.922	0.926	0.930	0.935	0.940	0.944	0.948	0.951	0.953	0.954	0.954	0.953	0.950	0.947	0.942	0.937	0.702
21	0.529	0.708	0.710	0.713	0.717	0.720	0.724	0.727	0.731	0.734	0.737	0.739	0.741	0.742	0.742	0.741	0.739	0.736	0.733	0.729	0.546

Inhomogeneity profile *hump 1* in OFE, local peak inhomogeneity factor of 1.06

	1	2	3	4	5	6	7	8	9	10	11	12	13	14
1	0.530	0.713	0.725	0.737	0.742	0.742	0.742	0.742	0.742	0.742	0.742	0.735	0.722	0.533
2	0.681	0.917	0.932	0.948	0.954	0.954	0.954	0.954	0.954	0.954	0.954	0.945	0.929	0.685
3	0.691	0.930	0.945	0.961	0.967	0.967	0.967	0.967	0.967	0.967	0.967	0.958	0.942	0.695
4	0.700	0.943	0.958	0.974	0.981	0.981	0.981	0.981	0.981	0.981	0.981	0.971	0.955	0.704
5	0.709	0.955	0.971	0.987	0.994	0.994	0.994	0.994	0.994	0.994	0.994	0.984	0.968	0.714
6	0.719	0.968	0.984	1.000	1.007	1.007	1.007	1.007	1.007	1.007	1.007	0.998	0.980	0.723
7	0.728	0.981	0.996	1.014	1.020	1.020	1.020	1.020	1.020	1.020	1.020	1.011	0.993	0.733
8	0.738	0.994	1.009	1.027	1.034	1.034	1.034	1.034	1.034	1.034	1.034	1.024	1.006	0.742
9	0.747	1.006	1.022	1.040	1.047	1.047	1.047	1.047	1.047	1.047	1.047	1.037	1.019	0.752
10	0.757	1.019	1.035	1.053	1.060	1.060	1.060	1.060	1.060	1.060	1.060	1.050	1.032	0.761
11	0.757	1.019	1.035	1.053	1.060	1.060	1.060	1.060	1.060	1.060	1.060	1.050	1.032	0.761
12	0.757	1.019	1.035	1.053	1.060	1.060	1.060	1.060	1.060	1.060	1.060	1.050	1.032	0.761
13	0.747	1.006	1.022	1.040	1.047	1.047	1.047	1.047	1.047	1.047	1.047	1.037	1.019	0.752
14	0.738	0.994	1.009	1.027	1.034	1.034	1.034	1.034	1.034	1.034	1.034	1.024	1.006	0.742
15	0.728	0.981	0.996	1.014	1.020	1.020	1.020	1.020	1.020	1.020	1.020	1.011	0.993	0.733
16	0.719	0.968	0.984	1.000	1.007	1.007	1.007	1.007	1.007	1.007	1.007	0.998	0.980	0.723
17	0.709	0.955	0.971	0.987	0.994	0.994	0.994	0.994	0.994	0.994	0.994	0.984	0.968	0.714
18	0.700	0.943	0.958	0.974	0.981	0.981	0.981	0.981	0.981	0.981	0.981	0.971	0.955	0.704
19	0.691	0.930	0.945	0.961	0.967	0.967	0.967	0.967	0.967	0.967	0.967	0.958	0.942	0.695
20	0.681	0.917	0.932	0.948	0.954	0.954	0.954	0.954	0.954	0.954	0.954	0.945	0.929	0.685
21	0.530	0.713	0.725	0.737	0.742	0.742	0.742	0.742	0.742	0.742	0.742	0.735	0.722	0.533

Inhomogeneity profile *hump 2* in IFE, local peak inhomogeneity factor of 1.12

	1	2	3	4	5	6	7	8	9	10	11	12	13	14	15	16	17	18	19	20	21
1	0.585	0.613	0.649	0.695	0.749	0.801	0.849	0.902	0.959	1.006	1.046	1.081	1.105	1.119	1.120	1.105	1.078	1.037	0.987	0.927	0.865
2	0.585	0.613	0.649	0.695	0.749	0.801	0.849	0.902	0.959	1.006	1.046	1.081	1.105	1.119	1.120	1.105	1.078	1.037	0.987	0.927	0.865
3	0.585	0.613	0.649	0.695	0.749	0.801	0.849	0.902	0.959	1.006	1.046	1.081	1.105	1.119	1.120	1.105	1.078	1.037	0.987	0.927	0.865
4	0.585	0.613	0.649	0.695	0.749	0.801	0.849	0.902	0.959	1.006	1.046	1.081	1.105	1.119	1.120	1.105	1.078	1.037	0.987	0.927	0.865
5	0.585	0.613	0.649	0.695	0.749	0.801	0.849	0.902	0.959	1.006	1.046	1.081	1.105	1.119	1.120	1.105	1.078	1.037	0.987	0.927	0.865
6	0.585	0.613	0.649	0.695	0.749	0.801	0.849	0.902	0.959	1.006	1.046	1.081	1.105	1.119	1.120	1.105	1.078	1.037	0.987	0.927	0.865
7	0.585	0.613	0.649	0.695	0.749	0.801	0.849	0.902	0.959	1.006	1.046	1.081	1.105	1.119	1.120	1.105	1.078	1.037	0.987	0.927	0.865
8	0.585	0.613	0.649	0.695	0.749	0.801	0.849	0.902	0.959	1.006	1.046	1.081	1.105	1.119	1.120	1.105	1.078	1.037	0.987	0.927	0.865
9	0.585	0.613	0.649	0.695	0.749	0.801	0.849	0.902	0.959	1.006	1.046	1.081	1.105	1.119	1.120	1.105	1.078	1.037	0.987	0.927	0.865
10	0.585	0.613	0.649	0.695	0.749	0.801	0.849	0.902	0.959	1.006	1.046	1.081	1.105	1.119	1.120	1.105	1.078	1.037	0.987	0.927	0.865
11	0.585	0.613	0.649	0.695	0.749	0.801	0.849	0.902	0.959	1.006	1.046	1.081	1.105	1.119	1.120	1.105	1.078	1.037	0.987	0.927	0.865
12	0.585	0.613	0.649	0.695	0.749	0.801	0.849	0.902	0.959	1.006	1.046	1.081	1.105	1.119	1.120	1.105	1.078	1.037	0.987	0.927	0.865
13	0.585	0.613	0.649	0.695	0.749	0.801	0.849	0.902	0.959	1.006	1.046	1.081	1.105	1.119	1.120	1.105	1.078	1.037	0.987	0.927	0.865
14	0.585	0.613	0.649	0.695	0.749	0.801	0.849	0.902	0.959	1.006	1.046	1.081	1.105	1.119	1.120	1.105	1.078	1.037	0.987	0.927	0.865
15	0.585	0.613	0.649	0.695	0.749	0.801	0.849	0.902	0.959	1.006	1.046	1.081	1.105	1.119	1.120	1.105	1.078	1.037	0.987	0.927	0.865
16	0.585	0.613	0.649	0.695	0.749	0.801	0.849	0.902	0.959	1.006	1.046	1.081	1.105	1.119	1.120	1.105	1.078	1.037	0.987	0.927	0.865
17	0.585	0.613	0.649	0.695	0.749	0.801	0.849	0.902	0.959	1.006	1.046	1.081	1.105	1.119	1.120	1.105	1.078	1.037	0.987	0.927	0.865
18	0.585	0.613	0.649	0.695	0.749	0.801	0.849	0.902	0.959	1.006	1.046	1.081	1.105	1.119	1.120	1.105	1.078	1.037	0.987	0.927	0.865
19	0.585	0.613	0.649	0.695	0.749	0.801	0.849	0.902	0.959	1.006	1.046	1.081	1.105	1.119	1.120	1.105	1.078	1.037	0.987	0.927	0.865
20	0.585	0.613	0.649	0.695	0.749	0.801	0.849	0.902	0.959	1.006	1.046	1.081	1.105	1.119	1.120	1.105	1.078	1.037	0.987	0.927	0.865
21	0.585	0.613	0.649	0.695	0.749	0.801	0.849	0.902	0.959	1.006	1.046	1.081	1.105	1.119	1.120	1.105	1.078	1.037	0.987	0.927	0.865

Inhomogeneity profile *hump 2* in OFE, local peak inhomogeneity factor of 1.12

	1	2	3	4	5	6	7	8	9	10	11	12	13	14
1	0.341	0.495	0.742	1.014	1.120	1.120	1.120	1.120	1.120	1.120	1.120	0.969	0.692	0.437
2	0.341	0.495	0.742	1.014	1.120	1.120	1.120	1.120	1.120	1.120	1.120	0.969	0.692	0.437
3	0.341	0.495	0.742	1.014	1.120	1.120	1.120	1.120	1.120	1.120	1.120	0.969	0.692	0.437
4	0.341	0.495	0.742	1.014	1.120	1.120	1.120	1.120	1.120	1.120	1.120	0.969	0.692	0.437
5	0.341	0.495	0.742	1.014	1.120	1.120	1.120	1.120	1.120	1.120	1.120	0.969	0.692	0.437
6	0.341	0.495	0.742	1.014	1.120	1.120	1.120	1.120	1.120	1.120	1.120	0.969	0.692	0.437
7	0.341	0.495	0.742	1.014	1.120	1.120	1.120	1.120	1.120	1.120	1.120	0.969	0.692	0.437
8	0.341	0.495	0.742	1.014	1.120	1.120	1.120	1.120	1.120	1.120	1.120	0.969	0.692	0.437
9	0.341	0.495	0.742	1.014	1.120	1.120	1.120	1.120	1.120	1.120	1.120	0.969	0.692	0.437
10	0.341	0.495	0.742	1.014	1.120	1.120	1.120	1.120	1.120	1.120	1.120	0.969	0.692	0.437
11	0.341	0.495	0.742	1.014	1.120	1.120	1.120	1.120	1.120	1.120	1.120	0.969	0.692	0.437
12	0.341	0.495	0.742	1.014	1.120	1.120	1.120	1.120	1.120	1.120	1.120	0.969	0.692	0.437
13	0.341	0.495	0.742	1.014	1.120	1.120	1.120	1.120	1.120	1.120	1.120	0.969	0.692	0.437
14	0.341	0.495	0.742	1.014	1.120	1.120	1.120	1.120	1.120	1.120	1.120	0.969	0.692	0.437
15	0.341	0.495	0.742	1.014	1.120	1.120	1.120	1.120	1.120	1.120	1.120	0.969	0.692	0.437
16	0.341	0.495	0.742	1.014	1.120	1.120	1.120	1.120	1.120	1.120	1.120	0.969	0.692	0.437
17	0.341	0.495	0.742	1.014	1.120	1.120	1.120	1.120	1.120	1.120	1.120	0.969	0.692	0.437
18	0.341	0.495	0.742	1.014	1.120	1.120	1.120	1.120	1.120	1.120	1.120	0.969	0.692	0.437
19	0.341	0.495	0.742	1.014	1.120	1.120	1.120	1.120	1.120	1.120	1.120	0.969	0.692	0.437
20	0.341	0.495	0.742	1.014	1.120	1.120	1.120	1.120	1.120	1.120	1.120	0.969	0.692	0.437
21	0.341	0.495	0.742	1.014	1.120	1.120	1.120	1.120	1.120	1.120	1.120	0.969	0.692	0.437

Inhomogeneity profile *hump 2* in IFE, local peak inhomogeneity factor of 1.09

	1	2	3	4	5	6	7	8	9	10	11	12	13	14	15	16	17	18	19	20	21
1	0.689	0.710	0.737	0.771	0.812	0.850	0.887	0.927	0.969	1.004	1.034	1.061	1.079	1.089	1.090	1.079	1.058	1.028	0.990	0.946	0.899
2	0.689	0.710	0.737	0.771	0.812	0.850	0.887	0.927	0.969	1.004	1.034	1.061	1.079	1.089	1.090	1.079	1.058	1.028	0.990	0.946	0.899
3	0.689	0.710	0.737	0.771	0.812	0.850	0.887	0.927	0.969	1.004	1.034	1.061	1.079	1.089	1.090	1.079	1.058	1.028	0.990	0.946	0.899
4	0.689	0.710	0.737	0.771	0.812	0.850	0.887	0.927	0.969	1.004	1.034	1.061	1.079	1.089	1.090	1.079	1.058	1.028	0.990	0.946	0.899
5	0.689	0.710	0.737	0.771	0.812	0.850	0.887	0.927	0.969	1.004	1.034	1.061	1.079	1.089	1.090	1.079	1.058	1.028	0.990	0.946	0.899
6	0.689	0.710	0.737	0.771	0.812	0.850	0.887	0.927	0.969	1.004	1.034	1.061	1.079	1.089	1.090	1.079	1.058	1.028	0.990	0.946	0.899
7	0.689	0.710	0.737	0.771	0.812	0.850	0.887	0.927	0.969	1.004	1.034	1.061	1.079	1.089	1.090	1.079	1.058	1.028	0.990	0.946	0.899
8	0.689	0.710	0.737	0.771	0.812	0.850	0.887	0.927	0.969	1.004	1.034	1.061	1.079	1.089	1.090	1.079	1.058	1.028	0.990	0.946	0.899
9	0.689	0.710	0.737	0.771	0.812	0.850	0.887	0.927	0.969	1.004	1.034	1.061	1.079	1.089	1.090	1.079	1.058	1.028	0.990	0.946	0.899
10	0.689	0.710	0.737	0.771	0.812	0.850	0.887	0.927	0.969	1.004	1.034	1.061	1.079	1.089	1.090	1.079	1.058	1.028	0.990	0.946	0.899
11	0.689	0.710	0.737	0.771	0.812	0.850	0.887	0.927	0.969	1.004	1.034	1.061	1.079	1.089	1.090	1.079	1.058	1.028	0.990	0.946	0.899
12	0.689	0.710	0.737	0.771	0.812	0.850	0.887	0.927	0.969	1.004	1.034	1.061	1.079	1.089	1.090	1.079	1.058	1.028	0.990	0.946	0.899
13	0.689	0.710	0.737	0.771	0.812	0.850	0.887	0.927	0.969	1.004	1.034	1.061	1.079	1.089	1.090	1.079	1.058	1.028	0.990	0.946	0.899
14	0.689	0.710	0.737	0.771	0.812	0.850	0.887	0.927	0.969	1.004	1.034	1.061	1.079	1.089	1.090	1.079	1.058	1.028	0.990	0.946	0.899
15	0.689	0.710	0.737	0.771	0.812	0.850	0.887	0.927	0.969	1.004	1.034	1.061	1.079	1.089	1.090	1.079	1.058	1.028	0.990	0.946	0.899
16	0.689	0.710	0.737	0.771	0.812	0.850	0.887	0.927	0.969	1.004	1.034	1.061	1.079	1.089	1.090	1.079	1.058	1.028	0.990	0.946	0.899
17	0.689	0.710	0.737	0.771	0.812	0.850	0.887	0.927	0.969	1.004	1.034	1.061	1.079	1.089	1.090	1.079	1.058	1.028	0.990	0.946	0.899
18	0.689	0.710	0.737	0.771	0.812	0.850	0.887	0.927	0.969	1.004	1.034	1.061	1.079	1.089	1.090	1.079	1.058	1.028	0.990	0.946	0.899
19	0.689	0.710	0.737	0.771	0.812	0.850	0.887	0.927	0.969	1.004	1.034	1.061	1.079	1.089	1.090	1.079	1.058	1.028	0.990	0.946	0.899
20	0.689	0.710	0.737	0.771	0.812	0.850	0.887	0.927	0.969	1.004	1.034	1.061	1.079	1.089	1.090	1.079	1.058	1.028	0.990	0.946	0.899
21	0.689	0.710	0.737	0.771	0.812	0.850	0.887	0.927	0.969	1.004	1.034	1.061	1.079	1.089	1.090	1.079	1.058	1.028	0.990	0.946	0.899

Inhomogeneity profile *hump 2* in OFE, local peak inhomogeneity factor of 1.09

	1	2	3	4	5	6	7	8	9	10	11	12	13	14
1	0.502	0.618	0.805	1.010	1.090	1.090	1.090	1.090	1.090	1.090	1.090	0.976	0.767	0.575
2	0.502	0.618	0.805	1.010	1.090	1.090	1.090	1.090	1.090	1.090	1.090	0.976	0.767	0.575
3	0.502	0.618	0.805	1.010	1.090	1.090	1.090	1.090	1.090	1.090	1.090	0.976	0.767	0.575
4	0.502	0.618	0.805	1.010	1.090	1.090	1.090	1.090	1.090	1.090	1.090	0.976	0.767	0.575
5	0.502	0.618	0.805	1.010	1.090	1.090	1.090	1.090	1.090	1.090	1.090	0.976	0.767	0.575
6	0.502	0.618	0.805	1.010	1.090	1.090	1.090	1.090	1.090	1.090	1.090	0.976	0.767	0.575
7	0.502	0.618	0.805	1.010	1.090	1.090	1.090	1.090	1.090	1.090	1.090	0.976	0.767	0.575
8	0.502	0.618	0.805	1.010	1.090	1.090	1.090	1.090	1.090	1.090	1.090	0.976	0.767	0.575
9	0.502	0.618	0.805	1.010	1.090	1.090	1.090	1.090	1.090	1.090	1.090	0.976	0.767	0.575
10	0.502	0.618	0.805	1.010	1.090	1.090	1.090	1.090	1.090	1.090	1.090	0.976	0.767	0.575
11	0.502	0.618	0.805	1.010	1.090	1.090	1.090	1.090	1.090	1.090	1.090	0.976	0.767	0.575
12	0.502	0.618	0.805	1.010	1.090	1.090	1.090	1.090	1.090	1.090	1.090	0.976	0.767	0.575
13	0.502	0.618	0.805	1.010	1.090	1.090	1.090	1.090	1.090	1.090	1.090	0.976	0.767	0.575
14	0.502	0.618	0.805	1.010	1.090	1.090	1.090	1.090	1.090	1.090	1.090	0.976	0.767	0.575
15	0.502	0.618	0.805	1.010	1.090	1.090	1.090	1.090	1.090	1.090	1.090	0.976	0.767	0.575
16	0.502	0.618	0.805	1.010	1.090	1.090	1.090	1.090	1.090	1.090	1.090	0.976	0.767	0.575
17	0.502	0.618	0.805	1.010	1.090	1.090	1.090	1.090	1.090	1.090	1.090	0.976	0.767	0.575
18	0.502	0.618	0.805	1.010	1.090	1.090	1.090	1.090	1.090	1.090	1.090	0.976	0.767	0.575
19	0.502	0.618	0.805	1.010	1.090	1.090	1.090	1.090	1.090	1.090	1.090	0.976	0.767	0.575
20	0.502	0.618	0.805	1.010	1.090	1.090	1.090	1.090	1.090	1.090	1.090	0.976	0.767	0.575
21	0.502	0.618	0.805	1.010	1.090	1.090	1.090	1.090	1.090	1.090	1.090	0.976	0.767	0.575

Inhomogeneity profile *hump 2* in IFE, local peak inhomogeneity factor of 1.06

	1	2	3	4	5	6	7	8	9	10	11	12	13	14	15	16	17	18	19	20	21
1	0.793	0.806	0.824	0.847	0.875	0.900	0.924	0.951	0.979	1.003	1.023	1.040	1.053	1.059	1.060	1.053	1.039	1.019	0.993	0.964	0.932
2	0.793	0.806	0.824	0.847	0.875	0.900	0.924	0.951	0.979	1.003	1.023	1.040	1.053	1.059	1.060	1.053	1.039	1.019	0.993	0.964	0.932
3	0.793	0.806	0.824	0.847	0.875	0.900	0.924	0.951	0.979	1.003	1.023	1.040	1.053	1.059	1.060	1.053	1.039	1.019	0.993	0.964	0.932
4	0.793	0.806	0.824	0.847	0.875	0.900	0.924	0.951	0.979	1.003	1.023	1.040	1.053	1.059	1.060	1.053	1.039	1.019	0.993	0.964	0.932
5	0.793	0.806	0.824	0.847	0.875	0.900	0.924	0.951	0.979	1.003	1.023	1.040	1.053	1.059	1.060	1.053	1.039	1.019	0.993	0.964	0.932
6	0.793	0.806	0.824	0.847	0.875	0.900	0.924	0.951	0.979	1.003	1.023	1.040	1.053	1.059	1.060	1.053	1.039	1.019	0.993	0.964	0.932
7	0.793	0.806	0.824	0.847	0.875	0.900	0.924	0.951	0.979	1.003	1.023	1.040	1.053	1.059	1.060	1.053	1.039	1.019	0.993	0.964	0.932
8	0.793	0.806	0.824	0.847	0.875	0.900	0.924	0.951	0.979	1.003	1.023	1.040	1.053	1.059	1.060	1.053	1.039	1.019	0.993	0.964	0.932
9	0.793	0.806	0.824	0.847	0.875	0.900	0.924	0.951	0.979	1.003	1.023	1.040	1.053	1.059	1.060	1.053	1.039	1.019	0.993	0.964	0.932
10	0.793	0.806	0.824	0.847	0.875	0.900	0.924	0.951	0.979	1.003	1.023	1.040	1.053	1.059	1.060	1.053	1.039	1.019	0.993	0.964	0.932
11	0.793	0.806	0.824	0.847	0.875	0.900	0.924	0.951	0.979	1.003	1.023	1.040	1.053	1.059	1.060	1.053	1.039	1.019	0.993	0.964	0.932
12	0.793	0.806	0.824	0.847	0.875	0.900	0.924	0.951	0.979	1.003	1.023	1.040	1.053	1.059	1.060	1.053	1.039	1.019	0.993	0.964	0.932
13	0.793	0.806	0.824	0.847	0.875	0.900	0.924	0.951	0.979	1.003	1.023	1.040	1.053	1.059	1.060	1.053	1.039	1.019	0.993	0.964	0.932
14	0.793	0.806	0.824	0.847	0.875	0.900	0.924	0.951	0.979	1.003	1.023	1.040	1.053	1.059	1.060	1.053	1.039	1.019	0.993	0.964	0.932
15	0.793	0.806	0.824	0.847	0.875	0.900	0.924	0.951	0.979	1.003	1.023	1.040	1.053	1.059	1.060	1.053	1.039	1.019	0.993	0.964	0.932
16	0.793	0.806	0.824	0.847	0.875	0.900	0.924	0.951	0.979	1.003	1.023	1.040	1.053	1.059	1.060	1.053	1.039	1.019	0.993	0.964	0.932
17	0.793	0.806	0.824	0.847	0.875	0.900	0.924	0.951	0.979	1.003	1.023	1.040	1.053	1.059	1.060	1.053	1.039	1.019	0.993	0.964	0.932
18	0.793	0.806	0.824	0.847	0.875	0.900	0.924	0.951	0.979	1.003	1.023	1.040	1.053	1.059	1.060	1.053	1.039	1.019	0.993	0.964	0.932
19	0.793	0.806	0.824	0.847	0.875	0.900	0.924	0.951	0.979	1.003	1.023	1.040	1.053	1.059	1.060	1.053	1.039	1.019	0.993	0.964	0.932
20	0.793	0.806	0.824	0.847	0.875	0.900	0.924	0.951	0.979	1.003	1.023	1.040	1.053	1.059	1.060	1.053	1.039	1.019	0.993	0.964	0.932
21	0.793	0.806	0.824	0.847	0.875	0.900	0.924	0.951	0.979	1.003	1.023	1.040	1.053	1.059	1.060	1.053	1.039	1.019	0.993	0.964	0.932

Inhomogeneity profile *hump 2* in OFE, local peak inhomogeneity factor of 1.06

	1	2	3	4	5	6	7	8	9	10	11	12	13	14
1	0.668	0.746	0.870	1.007	1.060	1.060	1.060	1.060	1.060	1.060	1.060	0.984	0.845	0.716
2	0.668	0.746	0.870	1.007	1.060	1.060	1.060	1.060	1.060	1.060	1.060	0.984	0.845	0.716
3	0.668	0.746	0.870	1.007	1.060	1.060	1.060	1.060	1.060	1.060	1.060	0.984	0.845	0.716
4	0.668	0.746	0.870	1.007	1.060	1.060	1.060	1.060	1.060	1.060	1.060	0.984	0.845	0.716
5	0.668	0.746	0.870	1.007	1.060	1.060	1.060	1.060	1.060	1.060	1.060	0.984	0.845	0.716
6	0.668	0.746	0.870	1.007	1.060	1.060	1.060	1.060	1.060	1.060	1.060	0.984	0.845	0.716
7	0.668	0.746	0.870	1.007	1.060	1.060	1.060	1.060	1.060	1.060	1.060	0.984	0.845	0.716
8	0.668	0.746	0.870	1.007	1.060	1.060	1.060	1.060	1.060	1.060	1.060	0.984	0.845	0.716
9	0.668	0.746	0.870	1.007	1.060	1.060	1.060	1.060	1.060	1.060	1.060	0.984	0.845	0.716
10	0.668	0.746	0.870	1.007	1.060	1.060	1.060	1.060	1.060	1.060	1.060	0.984	0.845	0.716
11	0.668	0.746	0.870	1.007	1.060	1.060	1.060	1.060	1.060	1.060	1.060	0.984	0.845	0.716
12	0.668	0.746	0.870	1.007	1.060	1.060	1.060	1.060	1.060	1.060	1.060	0.984	0.845	0.716
13	0.668	0.746	0.870	1.007	1.060	1.060	1.060	1.060	1.060	1.060	1.060	0.984	0.845	0.716
14	0.668	0.746	0.870	1.007	1.060	1.060	1.060	1.060	1.060	1.060	1.060	0.984	0.845	0.716
15	0.668	0.746	0.870	1.007	1.060	1.060	1.060	1.060	1.060	1.060	1.060	0.984	0.845	0.716
16	0.668	0.746	0.870	1.007	1.060	1.060	1.060	1.060	1.060	1.060	1.060	0.984	0.845	0.716
17	0.668	0.746	0.870	1.007	1.060	1.060	1.060	1.060	1.060	1.060	1.060	0.984	0.845	0.716
18	0.668	0.746	0.870	1.007	1.060	1.060	1.060	1.060	1.060	1.060	1.060	0.984	0.845	0.716
19	0.668	0.746	0.870	1.007	1.060	1.060	1.060	1.060	1.060	1.060	1.060	0.984	0.845	0.716
20	0.668	0.746	0.870	1.007	1.060	1.060	1.060	1.060	1.060	1.060	1.060	0.984	0.845	0.716
21	0.668	0.746	0.870	1.007	1.060	1.060	1.060	1.060	1.060	1.060	1.060	0.984	0.845	0.716

Inhomogeneity profile *edge 1* in IFE, local peak inhomogeneity factor of 1.12

	1	2	3	4	5	6	7	8	9	10	11	12	13	14	15	16	17	18	19	20	21
1	1.120	1.114	1.106	1.097	1.085	1.074	1.064	1.053	1.041	1.031	1.022	1.015	1.010	1.007	1.006	1.010	1.015	1.024	1.035	1.047	1.061
2	1.114	1.109	1.101	1.091	1.080	1.069	1.059	1.047	1.035	1.026	1.017	1.010	1.005	1.002	1.001	1.004	1.010	1.019	1.030	1.042	1.055
3	1.109	1.103	1.095	1.086	1.074	1.064	1.053	1.042	1.030	1.020	1.012	1.005	0.999	0.997	0.996	0.999	1.005	1.014	1.024	1.037	1.050
4	1.103	1.097	1.090	1.080	1.069	1.058	1.048	1.037	1.025	1.015	1.007	1.000	0.994	0.992	0.991	0.994	1.000	1.009	1.019	1.032	1.045
5	1.098	1.092	1.084	1.075	1.063	1.053	1.043	1.032	1.020	1.010	1.002	0.994	0.989	0.987	0.986	0.989	0.995	1.004	1.014	1.026	1.039
6	1.092	1.086	1.079	1.069	1.058	1.047	1.037	1.026	1.015	1.005	0.997	0.989	0.984	0.982	0.981	0.984	0.990	0.998	1.009	1.021	1.034
7	1.086	1.081	1.073	1.064	1.053	1.042	1.032	1.021	1.009	1.000	0.992	0.984	0.979	0.976	0.976	0.979	0.985	0.993	1.004	1.016	1.029
8	1.081	1.075	1.068	1.058	1.047	1.037	1.027	1.016	1.004	0.995	0.986	0.979	0.974	0.971	0.971	0.974	0.980	0.988	0.999	1.011	1.024
9	1.075	1.070	1.062	1.053	1.042	1.031	1.021	1.011	0.999	0.989	0.981	0.974	0.969	0.966	0.966	0.969	0.975	0.983	0.993	1.005	1.018
10	1.070	1.064	1.057	1.047	1.036	1.026	1.016	1.005	0.994	0.984	0.976	0.969	0.964	0.961	0.961	0.964	0.970	0.978	0.988	1.000	1.013
11	1.064	1.058	1.051	1.042	1.031	1.021	1.011	1.000	0.989	0.979	0.971	0.964	0.959	0.956	0.956	0.959	0.965	0.973	0.983	0.995	1.008
12	1.070	1.064	1.057	1.047	1.036	1.026	1.016	1.005	0.994	0.984	0.976	0.969	0.964	0.961	0.961	0.964	0.970	0.978	0.988	1.000	1.013
13	1.075	1.070	1.062	1.053	1.042	1.031	1.021	1.011	0.999	0.989	0.981	0.974	0.969	0.966	0.966	0.969	0.975	0.983	0.993	1.005	1.018
14	1.081	1.075	1.068	1.058	1.047	1.037	1.027	1.016	1.004	0.995	0.986	0.979	0.974	0.971	0.971	0.974	0.980	0.988	0.999	1.011	1.024
15	1.086	1.081	1.073	1.064	1.053	1.042	1.032	1.021	1.009	1.000	0.992	0.984	0.979	0.976	0.976	0.979	0.985	0.993	1.004	1.016	1.029
16	1.092	1.086	1.079	1.069	1.058	1.047	1.037	1.026	1.015	1.005	0.997	0.989	0.984	0.982	0.981	0.984	0.990	0.998	1.009	1.021	1.034
17	1.098	1.092	1.084	1.075	1.063	1.053	1.043	1.032	1.020	1.010	1.002	0.994	0.989	0.987	0.986	0.989	0.995	1.004	1.014	1.026	1.039
18	1.103	1.097	1.090	1.080	1.069	1.058	1.048	1.037	1.025	1.015	1.007	1.000	0.994	0.992	0.991	0.994	1.000	1.009	1.019	1.032	1.045
19	1.109	1.103	1.095	1.086	1.074	1.064	1.053	1.042	1.030	1.020	1.012	1.005	0.999	0.997	0.996	0.999	1.005	1.014	1.024	1.037	1.050
20	1.114	1.109	1.101	1.091	1.080	1.069	1.059	1.047	1.035	1.026	1.017	1.010	1.005	1.002	1.001	1.004	1.010	1.019	1.030	1.042	1.055
21	1.120	1.114	1.106	1.097	1.085	1.074	1.064	1.053	1.041	1.031	1.022	1.015	1.010	1.007	1.006	1.010	1.015	1.024	1.035	1.047	1.061

Inhomogeneity profile *edge 1* in OFE, local peak inhomogeneity factor of 1.12

	1	2	3	4	5	6	7	8	9	10	11	12	13	14
1	1.120	1.099	1.066	1.030	1.016	1.016	1.016	1.016	1.016	1.016	1.016	1.036	1.073	1.107
2	1.114	1.094	1.061	1.025	1.011	1.011	1.011	1.011	1.011	1.011	1.011	1.031	1.068	1.102
3	1.109	1.088	1.056	1.020	1.006	1.006	1.006	1.006	1.006	1.006	1.006	1.026	1.062	1.096
4	1.103	1.083	1.050	1.015	1.001	1.001	1.001	1.001	1.001	1.001	1.001	1.021	1.057	1.091
5	1.098	1.077	1.045	1.010	0.996	0.996	0.996	0.996	0.996	0.996	0.996	1.015	1.052	1.085
6	1.092	1.072	1.040	1.004	0.991	0.991	0.991	0.991	0.991	0.991	0.991	1.010	1.046	1.080
7	1.086	1.066	1.034	0.999	0.986	0.986	0.986	0.986	0.986	0.986	0.986	1.005	1.041	1.074
8	1.081	1.061	1.029	0.994	0.980	0.980	0.980	0.980	0.980	0.980	0.980	1.000	1.036	1.068
9	1.075	1.055	1.024	0.989	0.975	0.975	0.975	0.975	0.975	0.975	0.975	0.995	1.030	1.063
10	1.070	1.050	1.018	0.984	0.970	0.970	0.970	0.970	0.970	0.970	0.970	0.990	1.025	1.057
11	1.064	1.044	1.013	0.979	0.965	0.965	0.965	0.965	0.965	0.965	0.965	0.984	1.019	1.052
12	1.070	1.050	1.018	0.984	0.970	0.970	0.970	0.970	0.970	0.970	0.970	0.990	1.025	1.057
13	1.075	1.055	1.024	0.989	0.975	0.975	0.975	0.975	0.975	0.975	0.975	0.995	1.030	1.063
14	1.081	1.061	1.029	0.994	0.980	0.980	0.980	0.980	0.980	0.980	0.980	1.000	1.036	1.068
15	1.086	1.066	1.034	0.999	0.986	0.986	0.986	0.986	0.986	0.986	0.986	1.005	1.041	1.074
16	1.092	1.072	1.040	1.004	0.991	0.991	0.991	0.991	0.991	0.991	0.991	1.010	1.046	1.080
17	1.098	1.077	1.045	1.010	0.996	0.996	0.996	0.996	0.996	0.996	0.996	1.015	1.052	1.085
18	1.103	1.083	1.050	1.015	1.001	1.001	1.001	1.001	1.001	1.001	1.001	1.021	1.057	1.091
19	1.109	1.088	1.056	1.020	1.006	1.006	1.006	1.006	1.006	1.006	1.006	1.026	1.062	1.096
20	1.114	1.094	1.061	1.025	1.011	1.011	1.011	1.011	1.011	1.011	1.011	1.031	1.068	1.102
21	1.120	1.099	1.066	1.030	1.016	1.016	1.016	1.016	1.016	1.016	1.016	1.036	1.073	1.107

Inhomogeneity profile *edge 1* in IFE, local peak inhomogeneity factor of 1.09

	1	2	3	4	5	6	7	8	9	10	11	12	13	14	15	16	17	18	19	20	21
1	1.090	1.086	1.081	1.075	1.067	1.060	1.053	1.046	1.038	1.031	1.026	1.021	1.017	1.015	1.015	1.017	1.021	1.027	1.034	1.042	1.051
2	1.085	1.081	1.076	1.069	1.062	1.055	1.048	1.040	1.032	1.026	1.020	1.016	1.012	1.010	1.010	1.012	1.016	1.022	1.029	1.037	1.046
3	1.079	1.075	1.070	1.064	1.056	1.049	1.043	1.035	1.027	1.021	1.015	1.010	1.007	1.005	1.005	1.007	1.011	1.016	1.023	1.032	1.040
4	1.074	1.070	1.065	1.059	1.051	1.044	1.037	1.030	1.022	1.016	1.010	1.005	1.002	1.000	1.000	1.002	1.006	1.011	1.018	1.026	1.035
5	1.068	1.064	1.059	1.053	1.046	1.039	1.032	1.025	1.017	1.011	1.005	1.000	0.997	0.995	0.995	0.997	1.001	1.006	1.013	1.021	1.030
6	1.063	1.059	1.054	1.048	1.040	1.033	1.027	1.019	1.012	1.005	1.000	0.995	0.992	0.990	0.990	0.992	0.995	1.001	1.008	1.016	1.025
7	1.057	1.054	1.049	1.042	1.035	1.028	1.021	1.014	1.007	1.000	0.995	0.990	0.987	0.985	0.985	0.987	0.990	0.996	1.003	1.011	1.019
8	1.052	1.048	1.043	1.037	1.030	1.023	1.016	1.009	1.001	0.995	0.990	0.985	0.982	0.980	0.980	0.982	0.985	0.991	0.998	1.006	1.014
9	1.046	1.043	1.038	1.032	1.024	1.017	1.011	1.004	0.996	0.990	0.985	0.980	0.976	0.975	0.975	0.976	0.980	0.986	0.992	1.000	1.009
10	1.041	1.037	1.032	1.026	1.019	1.012	1.006	0.999	0.991	0.985	0.979	0.975	0.971	0.970	0.969	0.971	0.975	0.981	0.987	0.995	1.004
11	1.036	1.032	1.027	1.021	1.014	1.007	1.000	0.993	0.986	0.980	0.974	0.970	0.966	0.965	0.964	0.966	0.970	0.975	0.982	0.990	0.998
12	1.041	1.037	1.032	1.026	1.019	1.012	1.006	0.999	0.991	0.985	0.979	0.975	0.971	0.970	0.969	0.971	0.975	0.981	0.987	0.995	1.004
13	1.046	1.043	1.038	1.032	1.024	1.017	1.011	1.004	0.996	0.990	0.985	0.980	0.976	0.975	0.975	0.976	0.980	0.986	0.992	1.000	1.009
14	1.052	1.048	1.043	1.037	1.030	1.023	1.016	1.009	1.001	0.995	0.990	0.985	0.982	0.980	0.980	0.982	0.985	0.991	0.998	1.006	1.014
15	1.057	1.054	1.049	1.042	1.035	1.028	1.021	1.014	1.007	1.000	0.995	0.990	0.987	0.985	0.985	0.987	0.990	0.996	1.003	1.011	1.019
16	1.063	1.059	1.054	1.048	1.040	1.033	1.027	1.019	1.012	1.005	1.000	0.995	0.992	0.990	0.990	0.992	0.995	1.001	1.008	1.016	1.025
17	1.068	1.064	1.059	1.053	1.046	1.039	1.032	1.025	1.017	1.011	1.005	1.000	0.997	0.995	0.995	0.997	1.001	1.006	1.013	1.021	1.030
18	1.074	1.070	1.065	1.059	1.051	1.044	1.037	1.030	1.022	1.016	1.010	1.005	1.002	1.000	1.000	1.002	1.006	1.011	1.018	1.026	1.035
19	1.079	1.075	1.070	1.064	1.056	1.049	1.043	1.035	1.027	1.021	1.015	1.010	1.007	1.005	1.005	1.007	1.011	1.016	1.023	1.032	1.040
20	1.085	1.081	1.076	1.069	1.062	1.055	1.048	1.040	1.032	1.026	1.020	1.016	1.012	1.010	1.010	1.012	1.016	1.022	1.029	1.037	1.046
21	1.090	1.086	1.081	1.075	1.067	1.060	1.053	1.046	1.038	1.031	1.026	1.021	1.017	1.015	1.015	1.017	1.021	1.027	1.034	1.042	1.051

Inhomogeneity profile *edge 1* in OFE, local peak inhomogeneity factor of 1.09

	1	2	3	4	5	6	7	8	9	10	11	12	13	14
1	1.090	1.076	1.055	1.031	1.021	1.021	1.021	1.021	1.021	1.021	1.021	1.035	1.059	1.082
2	1.085	1.071	1.049	1.026	1.016	1.016	1.016	1.016	1.016	1.016	1.016	1.030	1.054	1.076
3	1.079	1.066	1.044	1.020	1.011	1.011	1.011	1.011	1.011	1.011	1.011	1.024	1.049	1.071
4	1.074	1.060	1.039	1.015	1.006	1.006	1.006	1.006	1.006	1.006	1.006	1.019	1.043	1.065
5	1.068	1.055	1.034	1.010	1.001	1.001	1.001	1.001	1.001	1.001	1.001	1.014	1.038	1.060
6	1.063	1.050	1.028	1.005	0.996	0.996	0.996	0.996	0.996	0.996	0.996	1.009	1.033	1.055
7	1.057	1.044	1.023	1.000	0.991	0.991	0.991	0.991	0.991	0.991	0.991	1.004	1.027	1.049
8	1.052	1.039	1.018	0.995	0.986	0.986	0.986	0.986	0.986	0.986	0.986	0.999	1.022	1.044
9	1.046	1.033	1.013	0.990	0.981	0.981	0.981	0.981	0.981	0.981	0.981	0.993	1.017	1.038
10	1.041	1.028	1.007	0.984	0.975	0.975	0.975	0.975	0.975	0.975	0.975	0.988	1.011	1.033
11	1.036	1.023	1.002	0.979	0.970	0.970	0.970	0.970	0.970	0.970	0.970	0.983	1.006	1.027
12	1.041	1.028	1.007	0.984	0.975	0.975	0.975	0.975	0.975	0.975	0.975	0.988	1.011	1.033
13	1.046	1.033	1.013	0.990	0.981	0.981	0.981	0.981	0.981	0.981	0.981	0.993	1.017	1.038
14	1.052	1.039	1.018	0.995	0.986	0.986	0.986	0.986	0.986	0.986	0.986	0.999	1.022	1.044
15	1.057	1.044	1.023	1.000	0.991	0.991	0.991	0.991	0.991	0.991	0.991	1.004	1.027	1.049
16	1.063	1.050	1.028	1.005	0.996	0.996	0.996	0.996	0.996	0.996	0.996	1.009	1.033	1.055
17	1.068	1.055	1.034	1.010	1.001	1.001	1.001	1.001	1.001	1.001	1.001	1.014	1.038	1.060
18	1.074	1.060	1.039	1.015	1.006	1.006	1.006	1.006	1.006	1.006	1.006	1.019	1.043	1.065
19	1.079	1.066	1.044	1.020	1.011	1.011	1.011	1.011	1.011	1.011	1.011	1.024	1.049	1.071
20	1.085	1.071	1.049	1.026	1.016	1.016	1.016	1.016	1.016	1.016	1.016	1.030	1.054	1.076
21	1.090	1.076	1.055	1.031	1.021	1.021	1.021	1.021	1.021	1.021	1.021	1.035	1.059	1.082

Inhomogeneity profile *edge 1* in IFE, local peak inhomogeneity factor of 1.06

	1	2	3	4	5	6	7	8	9	10	11	12	13	14	15	16	17	18	19	20	21
1	1.060	1.058	1.056	1.053	1.049	1.045	1.042	1.039	1.035	1.032	1.029	1.026	1.025	1.024	1.024	1.025	1.027	1.029	1.033	1.037	1.041
2	1.055	1.053	1.050	1.047	1.044	1.040	1.037	1.033	1.030	1.026	1.024	1.021	1.020	1.019	1.019	1.020	1.022	1.024	1.028	1.032	1.036
3	1.049	1.048	1.045	1.042	1.038	1.035	1.032	1.028	1.024	1.021	1.019	1.016	1.015	1.014	1.014	1.015	1.016	1.019	1.022	1.026	1.031
4	1.044	1.042	1.040	1.037	1.033	1.030	1.027	1.023	1.019	1.016	1.013	1.011	1.009	1.009	1.008	1.009	1.011	1.014	1.017	1.021	1.025
5	1.039	1.037	1.035	1.032	1.028	1.025	1.021	1.018	1.014	1.011	1.008	1.006	1.004	1.003	1.003	1.004	1.006	1.009	1.012	1.016	1.020
6	1.034	1.032	1.029	1.026	1.023	1.019	1.016	1.013	1.009	1.006	1.003	1.001	0.999	0.998	0.998	0.999	1.001	1.004	1.007	1.011	1.015
7	1.028	1.026	1.024	1.021	1.017	1.014	1.011	1.007	1.004	1.001	0.998	0.996	0.994	0.993	0.993	0.994	0.996	0.999	1.002	1.006	1.010
8	1.023	1.021	1.019	1.016	1.012	1.009	1.006	1.002	0.998	0.995	0.993	0.991	0.989	0.988	0.988	0.989	0.991	0.993	0.997	1.001	1.005
9	1.018	1.016	1.013	1.010	1.007	1.004	1.000	0.997	0.993	0.990	0.988	0.985	0.984	0.983	0.983	0.984	0.986	0.988	0.992	0.995	0.999
10	1.012	1.011	1.008	1.005	1.002	0.998	0.995	0.992	0.988	0.985	0.983	0.980	0.979	0.978	0.978	0.979	0.980	0.983	0.986	0.990	0.994
11	1.007	1.005	1.003	1.000	0.996	0.993	0.990	0.987	0.983	0.980	0.977	0.975	0.974	0.973	0.973	0.974	0.975	0.978	0.981	0.985	0.989
12	1.012	1.011	1.008	1.005	1.002	0.998	0.995	0.992	0.988	0.985	0.983	0.980	0.979	0.978	0.978	0.979	0.980	0.983	0.986	0.990	0.994
13	1.018	1.016	1.013	1.010	1.007	1.004	1.000	0.997	0.993	0.990	0.988	0.985	0.984	0.983	0.983	0.984	0.986	0.988	0.992	0.995	0.999
14	1.023	1.021	1.019	1.016	1.012	1.009	1.006	1.002	0.998	0.995	0.993	0.991	0.989	0.988	0.988	0.989	0.991	0.993	0.997	1.001	1.005
15	1.028	1.026	1.024	1.021	1.017	1.014	1.011	1.007	1.004	1.001	0.998	0.996	0.994	0.993	0.993	0.994	0.996	0.999	1.002	1.006	1.010
16	1.034	1.032	1.029	1.026	1.023	1.019	1.016	1.013	1.009	1.006	1.003	1.001	0.999	0.998	0.998	0.999	1.001	1.004	1.007	1.011	1.015
17	1.039	1.037	1.035	1.032	1.028	1.025	1.021	1.018	1.014	1.011	1.008	1.006	1.004	1.003	1.003	1.004	1.006	1.009	1.012	1.016	1.020
18	1.044	1.042	1.040	1.037	1.033	1.030	1.027	1.023	1.019	1.016	1.013	1.011	1.009	1.009	1.008	1.009	1.011	1.014	1.017	1.021	1.025
19	1.049	1.048	1.045	1.042	1.038	1.035	1.032	1.028	1.024	1.021	1.019	1.016	1.015	1.014	1.014	1.015	1.016	1.019	1.022	1.026	1.031
20	1.055	1.053	1.050	1.047	1.044	1.040	1.037	1.033	1.030	1.026	1.024	1.021	1.020	1.019	1.019	1.020	1.022	1.024	1.028	1.032	1.036
21	1.060	1.058	1.056	1.053	1.049	1.045	1.042	1.039	1.035	1.032	1.029	1.026	1.025	1.024	1.024	1.025	1.027	1.029	1.033	1.037	1.041

Inhomogeneity profile *edge 1* in OFE, local peak inhomogeneity factor of 1.06

	1	2	3	4	5	6	7	8	9	10	11	12	13	14
1	1.060	1.053	1.043	1.031	1.027	1.027	1.027	1.027	1.027	1.027	1.027	1.033	1.045	1.056
2	1.055	1.048	1.038	1.026	1.022	1.022	1.022	1.022	1.022	1.022	1.022	1.028	1.040	1.051
3	1.049	1.043	1.033	1.021	1.017	1.017	1.017	1.017	1.017	1.017	1.017	1.023	1.035	1.045
4	1.044	1.038	1.027	1.016	1.011	1.011	1.011	1.011	1.011	1.011	1.011	1.018	1.029	1.040
5	1.039	1.032	1.022	1.011	1.006	1.006	1.006	1.006	1.006	1.006	1.006	1.013	1.024	1.035
6	1.034	1.027	1.017	1.006	1.001	1.001	1.001	1.001	1.001	1.001	1.001	1.007	1.019	1.030
7	1.028	1.022	1.012	1.000	0.996	0.996	0.996	0.996	0.996	0.996	0.996	1.002	1.014	1.024
8	1.023	1.017	1.006	0.995	0.991	0.991	0.991	0.991	0.991	0.991	0.991	0.997	1.008	1.019
9	1.018	1.011	1.001	0.990	0.986	0.986	0.986	0.986	0.986	0.986	0.986	0.992	1.003	1.014
10	1.012	1.006	0.996	0.985	0.981	0.981	0.981	0.981	0.981	0.981	0.981	0.987	0.998	1.008
11	1.007	1.001	0.991	0.980	0.976	0.976	0.976	0.976	0.976	0.976	0.976	0.982	0.993	1.003
12	1.012	1.006	0.996	0.985	0.981	0.981	0.981	0.981	0.981	0.981	0.981	0.987	0.998	1.008
13	1.018	1.011	1.001	0.990	0.986	0.986	0.986	0.986	0.986	0.986	0.986	0.992	1.003	1.014
14	1.023	1.017	1.006	0.995	0.991	0.991	0.991	0.991	0.991	0.991	0.991	0.997	1.008	1.019
15	1.028	1.022	1.012	1.000	0.996	0.996	0.996	0.996	0.996	0.996	0.996	1.002	1.014	1.024
16	1.034	1.027	1.017	1.006	1.001	1.001	1.001	1.001	1.001	1.001	1.001	1.007	1.019	1.030
17	1.039	1.032	1.022	1.011	1.006	1.006	1.006	1.006	1.006	1.006	1.006	1.013	1.024	1.035
18	1.044	1.038	1.027	1.016	1.011	1.011	1.011	1.011	1.011	1.011	1.011	1.018	1.029	1.040
19	1.049	1.043	1.033	1.021	1.017	1.017	1.017	1.017	1.017	1.017	1.017	1.023	1.035	1.045
20	1.055	1.048	1.038	1.026	1.022	1.022	1.022	1.022	1.022	1.022	1.022	1.028	1.040	1.051
21	1.060	1.053	1.043	1.031	1.027	1.027	1.027	1.027	1.027	1.027	1.027	1.033	1.045	1.056

Inhomogeneity profile *edge 2* in IFE, local peak inhomogeneity factor of 1.12

	1	2	3	4	5	6	7	8	9	10	11	12	13	14	15	16	17	18	19	20	21
1	1.120	1.116	1.111	1.104	1.095	1.085	1.076	1.064	1.049	1.036	1.021	1.005	0.990	0.974	0.956	0.991	1.022	1.050	1.076	1.099	1.120
2	1.114	1.111	1.105	1.098	1.089	1.080	1.070	1.059	1.044	1.030	1.016	1.000	0.985	0.969	0.952	0.986	1.017	1.045	1.071	1.094	1.114
3	1.109	1.105	1.100	1.093	1.084	1.075	1.065	1.053	1.039	1.025	1.011	0.995	0.980	0.964	0.947	0.981	1.012	1.039	1.065	1.088	1.109
4	1.103	1.099	1.094	1.087	1.078	1.069	1.060	1.048	1.034	1.020	1.006	0.990	0.975	0.959	0.942	0.977	1.006	1.034	1.060	1.083	1.103
5	1.098	1.094	1.089	1.082	1.073	1.064	1.054	1.043	1.028	1.015	1.001	0.985	0.970	0.955	0.937	0.972	1.001	1.029	1.054	1.077	1.098
6	1.092	1.088	1.083	1.076	1.067	1.058	1.049	1.037	1.023	1.010	0.996	0.980	0.965	0.950	0.933	0.967	0.996	1.024	1.049	1.072	1.092
7	1.086	1.083	1.078	1.071	1.062	1.053	1.044	1.032	1.018	1.005	0.991	0.975	0.960	0.945	0.928	0.962	0.991	1.018	1.044	1.066	1.086
8	1.081	1.077	1.072	1.065	1.056	1.047	1.038	1.027	1.013	0.999	0.985	0.970	0.955	0.940	0.923	0.957	0.986	1.013	1.038	1.061	1.081
9	1.075	1.071	1.066	1.060	1.051	1.042	1.033	1.021	1.007	0.994	0.980	0.965	0.950	0.935	0.918	0.952	0.981	1.008	1.033	1.055	1.075
10	1.070	1.066	1.061	1.054	1.046	1.037	1.027	1.016	1.002	0.989	0.975	0.960	0.945	0.930	0.913	0.947	0.976	1.003	1.027	1.050	1.070
11	1.064	1.060	1.055	1.049	1.040	1.031	1.022	1.011	0.997	0.984	0.970	0.955	0.940	0.925	0.909	0.942	0.971	0.997	1.022	1.044	1.064
12	1.070	1.066	1.061	1.054	1.046	1.037	1.027	1.016	1.002	0.989	0.975	0.960	0.945	0.930	0.913	0.947	0.976	1.003	1.027	1.050	1.070
13	1.075	1.071	1.066	1.060	1.051	1.042	1.033	1.021	1.007	0.994	0.980	0.965	0.950	0.935	0.918	0.952	0.981	1.008	1.033	1.055	1.075
14	1.081	1.077	1.072	1.065	1.056	1.047	1.038	1.027	1.013	0.999	0.985	0.970	0.955	0.940	0.923	0.957	0.986	1.013	1.038	1.061	1.081
15	1.086	1.083	1.078	1.071	1.062	1.053	1.044	1.032	1.018	1.005	0.991	0.975	0.960	0.945	0.928	0.962	0.991	1.018	1.044	1.066	1.086
16	1.092	1.088	1.083	1.076	1.067	1.058	1.049	1.037	1.023	1.010	0.996	0.980	0.965	0.950	0.933	0.967	0.996	1.024	1.049	1.072	1.092
17	1.098	1.094	1.089	1.082	1.073	1.064	1.054	1.043	1.028	1.015	1.001	0.985	0.970	0.955	0.937	0.972	1.001	1.029	1.054	1.077	1.098
18	1.103	1.099	1.094	1.087	1.078	1.069	1.060	1.048	1.034	1.020	1.006	0.990	0.975	0.959	0.942	0.977	1.006	1.034	1.060	1.083	1.103
19	1.109	1.105	1.100	1.093	1.084	1.075	1.065	1.053	1.039	1.025	1.011	0.995	0.980	0.964	0.947	0.981	1.012	1.039	1.065	1.088	1.109
20	1.114	1.111	1.105	1.098	1.089	1.080	1.070	1.059	1.044	1.030	1.016	1.000	0.985	0.969	0.952	0.986	1.017	1.045	1.071	1.094	1.114
21	1.120	1.116	1.111	1.104	1.095	1.085	1.076	1.064	1.049	1.036	1.021	1.005	0.990	0.974	0.956	0.991	1.022	1.050	1.076	1.099	1.120

Inhomogeneity profile *edge 2* in OFE, local peak inhomogeneity factor of 1.12

	1	2	3	4	5	6	7	8	9	10	11	12	13	14
1	1.120	1.110	1.092	1.064	1.036	1.007	0.977	0.946	0.978	1.010	1.044	1.078	1.104	1.120
2	1.114	1.105	1.086	1.059	1.031	1.002	0.972	0.941	0.973	1.005	1.038	1.072	1.098	1.114
3	1.109	1.099	1.081	1.053	1.026	0.997	0.967	0.937	0.968	1.000	1.033	1.067	1.093	1.109
4	1.103	1.094	1.075	1.048	1.020	0.992	0.962	0.932	0.963	0.995	1.028	1.062	1.087	1.103
5	1.098	1.088	1.070	1.043	1.015	0.987	0.957	0.927	0.958	0.990	1.023	1.056	1.082	1.098
6	1.092	1.083	1.064	1.038	1.010	0.982	0.952	0.923	0.953	0.985	1.018	1.051	1.076	1.092
7	1.086	1.077	1.059	1.032	1.005	0.977	0.948	0.918	0.948	0.980	1.012	1.045	1.071	1.086
8	1.081	1.072	1.053	1.027	1.000	0.972	0.943	0.913	0.944	0.975	1.007	1.040	1.065	1.081
9	1.075	1.066	1.048	1.022	0.994	0.967	0.938	0.908	0.939	0.970	1.002	1.035	1.060	1.075
10	1.070	1.060	1.042	1.016	0.989	0.962	0.933	0.904	0.934	0.965	0.997	1.029	1.054	1.070
11	1.064	1.055	1.037	1.011	0.984	0.956	0.928	0.899	0.929	0.960	0.991	1.024	1.049	1.064
12	1.070	1.060	1.042	1.016	0.989	0.962	0.933	0.904	0.934	0.965	0.997	1.029	1.054	1.070
13	1.075	1.066	1.048	1.022	0.994	0.967	0.938	0.908	0.939	0.970	1.002	1.035	1.060	1.075
14	1.081	1.072	1.053	1.027	1.000	0.972	0.943	0.913	0.944	0.975	1.007	1.040	1.065	1.081
15	1.086	1.077	1.059	1.032	1.005	0.977	0.948	0.918	0.948	0.980	1.012	1.045	1.071	1.086
16	1.092	1.083	1.064	1.038	1.010	0.982	0.952	0.923	0.953	0.985	1.018	1.051	1.076	1.092
17	1.098	1.088	1.070	1.043	1.015	0.987	0.957	0.927	0.958	0.990	1.023	1.056	1.082	1.098
18	1.103	1.094	1.075	1.048	1.020	0.992	0.962	0.932	0.963	0.995	1.028	1.062	1.087	1.103
19	1.109	1.099	1.081	1.053	1.026	0.997	0.967	0.937	0.968	1.000	1.033	1.067	1.093	1.109
20	1.114	1.105	1.086	1.059	1.031	1.002	0.972	0.941	0.973	1.005	1.038	1.072	1.098	1.114
21	1.120	1.110	1.092	1.064	1.036	1.007	0.977	0.946	0.978	1.010	1.044	1.078	1.104	1.120

Inhomogeneity profile *edge 2* in IFE, local peak inhomogeneity factor of 1.09

	1	2	3	4	5	6	7	8	9	10	11	12	13	14	15	16	17	18	19	20	21
1	1.090	1.087	1.084	1.079	1.073	1.067	1.061	1.053	1.043	1.034	1.025	1.014	1.004	0.994	0.982	1.005	1.025	1.044	1.061	1.076	1.090
2	1.085	1.082	1.079	1.074	1.068	1.062	1.056	1.048	1.038	1.029	1.020	1.009	0.999	0.989	0.977	1.000	1.020	1.039	1.056	1.071	1.085
3	1.079	1.077	1.073	1.069	1.063	1.057	1.050	1.042	1.033	1.024	1.015	1.004	0.994	0.984	0.972	0.995	1.015	1.033	1.050	1.066	1.079
4	1.074	1.071	1.068	1.063	1.057	1.051	1.045	1.037	1.028	1.019	1.009	0.999	0.989	0.979	0.967	0.990	1.010	1.028	1.045	1.060	1.074
5	1.068	1.066	1.062	1.058	1.052	1.046	1.040	1.032	1.023	1.014	1.004	0.994	0.984	0.974	0.962	0.985	1.005	1.023	1.040	1.055	1.068
6	1.063	1.060	1.057	1.052	1.047	1.041	1.034	1.027	1.017	1.008	0.999	0.989	0.979	0.969	0.958	0.980	1.000	1.018	1.034	1.049	1.063
7	1.057	1.055	1.052	1.047	1.041	1.035	1.029	1.021	1.012	1.003	0.994	0.984	0.974	0.964	0.953	0.975	0.994	1.013	1.029	1.044	1.057
8	1.052	1.049	1.046	1.042	1.036	1.030	1.024	1.016	1.007	0.998	0.989	0.979	0.969	0.959	0.948	0.970	0.989	1.007	1.024	1.039	1.052
9	1.046	1.044	1.041	1.036	1.030	1.025	1.018	1.011	1.002	0.993	0.984	0.974	0.964	0.954	0.943	0.965	0.984	1.002	1.018	1.033	1.046
10	1.041	1.039	1.035	1.031	1.025	1.019	1.013	1.006	0.997	0.988	0.979	0.969	0.959	0.949	0.938	0.960	0.979	0.997	1.013	1.028	1.041
11	1.036	1.033	1.030	1.025	1.020	1.014	1.008	1.000	0.991	0.983	0.974	0.964	0.954	0.944	0.933	0.955	0.974	0.992	1.008	1.023	1.036
12	1.041	1.039	1.035	1.031	1.025	1.019	1.013	1.006	0.997	0.988	0.979	0.969	0.959	0.949	0.938	0.960	0.979	0.997	1.013	1.028	1.041
13	1.046	1.044	1.041	1.036	1.030	1.025	1.018	1.011	1.002	0.993	0.984	0.974	0.964	0.954	0.943	0.965	0.984	1.002	1.018	1.033	1.046
14	1.052	1.049	1.046	1.042	1.036	1.030	1.024	1.016	1.007	0.998	0.989	0.979	0.969	0.959	0.948	0.970	0.989	1.007	1.024	1.039	1.052
15	1.057	1.055	1.052	1.047	1.041	1.035	1.029	1.021	1.012	1.003	0.994	0.984	0.974	0.964	0.953	0.975	0.994	1.013	1.029	1.044	1.057
16	1.063	1.060	1.057	1.052	1.047	1.041	1.034	1.027	1.017	1.008	0.999	0.989	0.979	0.969	0.958	0.980	1.000	1.018	1.034	1.049	1.063
17	1.068	1.066	1.062	1.058	1.052	1.046	1.040	1.032	1.023	1.014	1.004	0.994	0.984	0.974	0.962	0.985	1.005	1.023	1.040	1.055	1.068
18	1.074	1.071	1.068	1.063	1.057	1.051	1.045	1.037	1.028	1.019	1.009	0.999	0.989	0.979	0.967	0.990	1.010	1.028	1.045	1.060	1.074
19	1.079	1.077	1.073	1.069	1.063	1.057	1.050	1.042	1.033	1.024	1.015	1.004	0.994	0.984	0.972	0.995	1.015	1.033	1.050	1.066	1.079
20	1.085	1.082	1.079	1.074	1.068	1.062	1.056	1.048	1.038	1.029	1.020	1.009	0.999	0.989	0.977	1.000	1.020	1.039	1.056	1.071	1.085
21	1.090	1.087	1.084	1.079	1.073	1.067	1.061	1.053	1.043	1.034	1.025	1.014	1.004	0.994	0.982	1.005	1.025	1.044	1.061	1.076	1.090

Inhomogeneity profile *edge 2* in OFE, local peak inhomogeneity factor of 1.09

	1	2	3	4	5	6	7	8	9	10	11	12	13	14
1	1.090	1.084	1.071	1.053	1.035	1.015	0.996	0.975	0.996	1.018	1.040	1.062	1.079	1.090
2	1.085	1.078	1.066	1.048	1.029	1.010	0.991	0.971	0.991	1.013	1.034	1.057	1.074	1.085
3	1.079	1.073	1.061	1.043	1.024	1.005	0.986	0.966	0.986	1.007	1.029	1.052	1.069	1.079
4	1.074	1.067	1.055	1.037	1.019	1.000	0.981	0.961	0.981	1.002	1.024	1.046	1.063	1.074
5	1.068	1.062	1.050	1.032	1.014	0.995	0.976	0.956	0.976	0.997	1.019	1.041	1.058	1.068
6	1.063	1.057	1.044	1.027	1.009	0.990	0.971	0.951	0.971	0.992	1.014	1.036	1.052	1.063
7	1.057	1.051	1.039	1.022	1.004	0.985	0.966	0.946	0.966	0.987	1.008	1.030	1.047	1.057
8	1.052	1.046	1.034	1.016	0.998	0.980	0.961	0.941	0.961	0.982	1.003	1.025	1.042	1.052
9	1.046	1.040	1.028	1.011	0.993	0.975	0.956	0.936	0.956	0.977	0.998	1.020	1.036	1.046
10	1.041	1.035	1.023	1.006	0.988	0.970	0.951	0.932	0.951	0.972	0.993	1.014	1.031	1.041
11	1.036	1.030	1.018	1.001	0.983	0.965	0.946	0.927	0.946	0.967	0.988	1.009	1.025	1.036
12	1.041	1.035	1.023	1.006	0.988	0.970	0.951	0.932	0.951	0.972	0.993	1.014	1.031	1.041
13	1.046	1.040	1.028	1.011	0.993	0.975	0.956	0.936	0.956	0.977	0.998	1.020	1.036	1.046
14	1.052	1.046	1.034	1.016	0.998	0.980	0.961	0.941	0.961	0.982	1.003	1.025	1.042	1.052
15	1.057	1.051	1.039	1.022	1.004	0.985	0.966	0.946	0.966	0.987	1.008	1.030	1.047	1.057
16	1.063	1.057	1.044	1.027	1.009	0.990	0.971	0.951	0.971	0.992	1.014	1.036	1.052	1.063
17	1.068	1.062	1.050	1.032	1.014	0.995	0.976	0.956	0.976	0.997	1.019	1.041	1.058	1.068
18	1.074	1.067	1.055	1.037	1.019	1.000	0.981	0.961	0.981	1.002	1.024	1.046	1.063	1.074
19	1.079	1.073	1.061	1.043	1.024	1.005	0.986	0.966	0.986	1.007	1.029	1.052	1.069	1.079
20	1.085	1.078	1.066	1.048	1.029	1.010	0.991	0.971	0.991	1.013	1.034	1.057	1.074	1.085
21	1.090	1.084	1.071	1.053	1.035	1.015	0.996	0.975	0.996	1.018	1.040	1.062	1.079	1.090

Inhomogeneity profile *edge 2* in IFE, local peak inhomogeneity factor of 1.06

	1	2	3	4	5	6	7	8	9	10	11	12	13	14	15	16	17	18	19	20	21
1	1.060	1.059	1.057	1.055	1.052	1.049	1.046	1.042	1.038	1.033	1.029	1.023	1.019	1.013	1.008	1.019	1.029	1.038	1.046	1.053	1.060
2	1.055	1.053	1.052	1.050	1.047	1.044	1.041	1.037	1.032	1.028	1.023	1.018	1.013	1.008	1.003	1.014	1.024	1.032	1.041	1.048	1.055
3	1.049	1.048	1.047	1.044	1.041	1.038	1.035	1.032	1.027	1.023	1.018	1.013	1.008	1.003	0.998	1.009	1.018	1.027	1.035	1.043	1.049
4	1.044	1.043	1.041	1.039	1.036	1.033	1.030	1.026	1.022	1.018	1.013	1.008	1.003	0.998	0.993	1.004	1.013	1.022	1.030	1.038	1.044
5	1.039	1.038	1.036	1.034	1.031	1.028	1.025	1.021	1.017	1.012	1.008	1.003	0.998	0.993	0.988	0.999	1.008	1.017	1.025	1.032	1.039
6	1.034	1.032	1.031	1.028	1.026	1.023	1.020	1.016	1.012	1.007	1.003	0.998	0.993	0.988	0.983	0.994	1.003	1.012	1.020	1.027	1.034
7	1.028	1.027	1.025	1.023	1.020	1.018	1.015	1.011	1.006	1.002	0.998	0.993	0.988	0.983	0.978	0.988	0.998	1.007	1.015	1.022	1.028
8	1.023	1.022	1.020	1.018	1.015	1.012	1.009	1.006	1.001	0.997	0.993	0.988	0.983	0.978	0.973	0.983	0.993	1.001	1.009	1.017	1.023
9	1.018	1.016	1.015	1.013	1.010	1.007	1.004	1.000	0.996	0.992	0.987	0.982	0.978	0.973	0.968	0.978	0.988	0.996	1.004	1.011	1.018
10	1.012	1.011	1.010	1.007	1.005	1.002	0.999	0.995	0.991	0.987	0.982	0.977	0.973	0.968	0.962	0.973	0.982	0.991	0.999	1.006	1.012
11	1.007	1.006	1.004	1.002	0.999	0.997	0.994	0.990	0.986	0.981	0.977	0.972	0.968	0.963	0.957	0.968	0.977	0.986	0.994	1.001	1.007
12	1.012	1.011	1.010	1.007	1.005	1.002	0.999	0.995	0.991	0.987	0.982	0.977	0.973	0.968	0.962	0.973	0.982	0.991	0.999	1.006	1.012
13	1.018	1.016	1.015	1.013	1.010	1.007	1.004	1.000	0.996	0.992	0.987	0.982	0.978	0.973	0.968	0.978	0.988	0.996	1.004	1.011	1.018
14	1.023	1.022	1.020	1.018	1.015	1.012	1.009	1.006	1.001	0.997	0.993	0.988	0.983	0.978	0.973	0.983	0.993	1.001	1.009	1.017	1.023
15	1.028	1.027	1.025	1.023	1.020	1.018	1.015	1.011	1.006	1.002	0.998	0.993	0.988	0.983	0.978	0.988	0.998	1.007	1.015	1.022	1.028
16	1.034	1.032	1.031	1.028	1.026	1.023	1.020	1.016	1.012	1.007	1.003	0.998	0.993	0.988	0.983	0.994	1.003	1.012	1.020	1.027	1.034
17	1.039	1.038	1.036	1.034	1.031	1.028	1.025	1.021	1.017	1.012	1.008	1.003	0.998	0.993	0.988	0.999	1.008	1.017	1.025	1.032	1.039
18	1.044	1.043	1.041	1.039	1.036	1.033	1.030	1.026	1.022	1.018	1.013	1.008	1.003	0.998	0.993	1.004	1.013	1.022	1.030	1.038	1.044
19	1.049	1.048	1.047	1.044	1.041	1.038	1.035	1.032	1.027	1.023	1.018	1.013	1.008	1.003	0.998	1.009	1.018	1.027	1.035	1.043	1.049
20	1.055	1.053	1.052	1.050	1.047	1.044	1.041	1.037	1.032	1.028	1.023	1.018	1.013	1.008	1.003	1.014	1.024	1.032	1.041	1.048	1.055
21	1.060	1.059	1.057	1.055	1.052	1.049	1.046	1.042	1.038	1.033	1.029	1.023	1.019	1.013	1.008	1.019	1.029	1.038	1.046	1.053	1.060

Inhomogeneity profile *edge 2* in OFE, local peak inhomogeneity factor of 1.06

	1	2	3	4	5	6	7	8	9	10	11	12	13	14
1	1.060	1.057	1.051	1.042	1.033	1.024	1.014	1.005	1.015	1.025	1.036	1.047	1.055	1.060
2	1.055	1.052	1.046	1.037	1.028	1.019	1.009	1.000	1.010	1.020	1.030	1.041	1.050	1.055
3	1.049	1.046	1.040	1.032	1.023	1.014	1.004	0.995	1.005	1.015	1.025	1.036	1.044	1.049
4	1.044	1.041	1.035	1.027	1.018	1.009	0.999	0.990	0.999	1.010	1.020	1.031	1.039	1.044
5	1.039	1.036	1.030	1.021	1.013	1.003	0.994	0.985	0.994	1.005	1.015	1.026	1.034	1.039
6	1.034	1.031	1.025	1.016	1.007	0.998	0.989	0.980	0.989	0.999	1.010	1.020	1.028	1.034
7	1.028	1.025	1.019	1.011	1.002	0.993	0.984	0.974	0.984	0.994	1.005	1.015	1.023	1.028
8	1.023	1.020	1.014	1.006	0.997	0.988	0.979	0.969	0.979	0.989	0.999	1.010	1.018	1.023
9	1.018	1.015	1.009	1.001	0.992	0.983	0.974	0.964	0.974	0.984	0.994	1.005	1.013	1.018
10	1.012	1.009	1.004	0.995	0.987	0.978	0.969	0.959	0.969	0.979	0.989	0.999	1.007	1.012
11	1.007	1.004	0.998	0.990	0.982	0.973	0.964	0.954	0.964	0.974	0.984	0.994	1.002	1.007
12	1.012	1.009	1.004	0.995	0.987	0.978	0.969	0.959	0.969	0.979	0.989	0.999	1.007	1.012
13	1.018	1.015	1.009	1.001	0.992	0.983	0.974	0.964	0.974	0.984	0.994	1.005	1.013	1.018
14	1.023	1.020	1.014	1.006	0.997	0.988	0.979	0.969	0.979	0.989	0.999	1.010	1.018	1.023
15	1.028	1.025	1.019	1.011	1.002	0.993	0.984	0.974	0.984	0.994	1.005	1.015	1.023	1.028
16	1.034	1.031	1.025	1.016	1.007	0.998	0.989	0.980	0.989	0.999	1.010	1.020	1.028	1.034
17	1.039	1.036	1.030	1.021	1.013	1.003	0.994	0.985	0.994	1.005	1.015	1.026	1.034	1.039
18	1.044	1.041	1.035	1.027	1.018	1.009	0.999	0.990	0.999	1.010	1.020	1.031	1.039	1.044
19	1.049	1.046	1.040	1.032	1.023	1.014	1.004	0.995	1.005	1.015	1.025	1.036	1.044	1.049
20	1.055	1.052	1.046	1.037	1.028	1.019	1.009	1.000	1.010	1.020	1.030	1.041	1.050	1.055
21	1.060	1.057	1.051	1.042	1.033	1.024	1.014	1.005	1.015	1.025	1.036	1.047	1.055	1.060

Inhomogeneity profile *edge 3* in IFE, local peak inhomogeneity factor of 1.12

	1	2	3	4	5	6	7	8	9	10	11	12	13	14	15	16	17	18	19	20	21
1	1.120	1.120	1.120	1.120	1.120	1.120	1.120	1.120	1.120	1.120	1.120	1.120	1.120	1.120	1.120	1.120	1.120	1.120	1.120	1.120	1.120
2	1.120	1.120	1.120	1.119	1.119	1.118	1.118	1.117	1.117	1.116	1.115	1.114	1.114	1.113	1.112	1.114	1.115	1.117	1.118	1.119	1.120
3	1.120	1.120	1.119	1.118	1.117	1.116	1.115	1.113	1.111	1.110	1.108	1.106	1.104	1.102	1.100	1.104	1.108	1.111	1.115	1.117	1.120
4	1.120	1.119	1.118	1.116	1.114	1.112	1.110	1.108	1.104	1.101	1.098	1.095	1.091	1.088	1.084	1.092	1.098	1.105	1.110	1.115	1.120
5	1.120	1.119	1.117	1.114	1.111	1.107	1.104	1.100	1.094	1.089	1.084	1.078	1.072	1.067	1.060	1.073	1.084	1.094	1.104	1.112	1.120
6	1.120	1.117	1.114	1.109	1.102	1.096	1.089	1.080	1.070	1.060	1.050	1.039	1.028	1.017	1.005	1.029	1.051	1.071	1.089	1.105	1.120
7	1.120	1.115	1.109	1.101	1.090	1.079	1.067	1.053	1.036	1.019	1.002	0.983	0.964	0.945	0.924	0.966	1.002	1.036	1.067	1.095	1.120
8	1.120	1.113	1.105	1.093	1.077	1.062	1.045	1.025	1.001	0.978	0.953	0.926	0.900	0.874	0.844	0.903	0.954	1.002	1.046	1.085	1.120
9	1.120	1.112	1.100	1.085	1.065	1.045	1.024	0.998	0.966	0.936	0.905	0.870	0.837	0.802	0.764	0.840	0.906	0.967	1.024	1.075	1.120
10	1.120	1.110	1.097	1.079	1.056	1.033	1.009	0.978	0.942	0.907	0.871	0.831	0.792	0.752	0.707	0.796	0.872	0.943	1.009	1.068	1.120
11	1.120	1.109	1.095	1.076	1.051	1.026	1.000	0.967	0.928	0.891	0.851	0.808	0.766	0.723	0.675	0.770	0.853	0.930	1.000	1.064	1.120
12	1.120	1.110	1.097	1.079	1.056	1.033	1.009	0.978	0.942	0.907	0.871	0.831	0.792	0.752	0.707	0.796	0.872	0.943	1.009	1.068	1.120
13	1.120	1.112	1.100	1.085	1.065	1.045	1.024	0.998	0.966	0.936	0.905	0.870	0.837	0.802	0.764	0.840	0.906	0.967	1.024	1.075	1.120
14	1.120	1.113	1.105	1.093	1.077	1.062	1.045	1.025	1.001	0.978	0.953	0.926	0.900	0.874	0.844	0.903	0.954	1.002	1.046	1.085	1.120
15	1.120	1.115	1.109	1.101	1.090	1.079	1.067	1.053	1.036	1.019	1.002	0.983	0.964	0.945	0.924	0.966	1.002	1.036	1.067	1.095	1.120
16	1.120	1.117	1.114	1.109	1.102	1.096	1.089	1.080	1.070	1.060	1.050	1.039	1.028	1.017	1.005	1.029	1.051	1.071	1.089	1.105	1.120
17	1.120	1.119	1.117	1.114	1.111	1.107	1.104	1.100	1.094	1.089	1.084	1.078	1.072	1.067	1.060	1.073	1.084	1.094	1.104	1.112	1.120
18	1.120	1.119	1.118	1.116	1.114	1.112	1.110	1.108	1.104	1.101	1.098	1.095	1.091	1.088	1.084	1.092	1.098	1.105	1.110	1.115	1.120
19	1.120	1.120	1.119	1.118	1.117	1.116	1.115	1.113	1.111	1.110	1.108	1.106	1.104	1.102	1.100	1.104	1.108	1.111	1.115	1.117	1.120
20	1.120	1.120	1.120	1.119	1.119	1.118	1.118	1.117	1.117	1.116	1.115	1.114	1.114	1.113	1.112	1.114	1.115	1.117	1.118	1.119	1.120
21	1.120	1.120	1.120	1.120	1.120	1.120	1.120	1.120	1.120	1.120	1.120	1.120	1.120	1.120	1.120	1.120	1.120	1.120	1.120	1.120	1.120

Inhomogeneity profile *edge 3* in OFE, local peak inhomogeneity factor of 1.12

	1	2	3	4	5	6	7	8	9	10	11	12	13	14
1	1.120	1.120	1.120	1.120	1.120	1.120	1.120	1.120	1.120	1.120	1.120	1.120	1.120	1.120
2	1.120	1.120	1.119	1.117	1.116	1.114	1.113	1.111	1.113	1.115	1.116	1.118	1.119	1.120
3	1.120	1.119	1.117	1.113	1.110	1.106	1.102	1.099	1.103	1.107	1.111	1.115	1.118	1.120
4	1.120	1.118	1.114	1.108	1.101	1.095	1.088	1.082	1.089	1.096	1.103	1.111	1.116	1.120
5	1.120	1.117	1.110	1.100	1.089	1.079	1.068	1.057	1.068	1.080	1.092	1.105	1.114	1.120
6	1.120	1.113	1.100	1.081	1.061	1.040	1.019	0.997	1.020	1.043	1.066	1.090	1.109	1.120
7	1.120	1.109	1.086	1.053	1.019	0.985	0.949	0.912	0.950	0.989	1.029	1.069	1.101	1.120
8	1.120	1.104	1.072	1.026	0.978	0.929	0.879	0.827	0.880	0.935	0.991	1.049	1.093	1.120
9	1.120	1.099	1.058	0.998	0.937	0.874	0.808	0.741	0.810	0.881	0.954	1.028	1.085	1.120
10	1.120	1.096	1.048	0.979	0.908	0.835	0.759	0.682	0.762	0.843	0.927	1.014	1.079	1.120
11	1.120	1.094	1.043	0.968	0.891	0.812	0.731	0.648	0.734	0.822	0.912	1.005	1.076	1.120
12	1.120	1.096	1.048	0.979	0.908	0.835	0.759	0.682	0.762	0.843	0.927	1.014	1.079	1.120
13	1.120	1.099	1.058	0.998	0.937	0.874	0.808	0.741	0.810	0.881	0.954	1.028	1.085	1.120
14	1.120	1.104	1.072	1.026	0.978	0.929	0.879	0.827	0.880	0.935	0.991	1.049	1.093	1.120
15	1.120	1.109	1.086	1.053	1.019	0.985	0.949	0.912	0.950	0.989	1.029	1.069	1.101	1.120
16	1.120	1.113	1.100	1.081	1.061	1.040	1.019	0.997	1.020	1.043	1.066	1.090	1.109	1.120
17	1.120	1.117	1.110	1.100	1.089	1.079	1.068	1.057	1.068	1.080	1.092	1.105	1.114	1.120
18	1.120	1.118	1.114	1.108	1.101	1.095	1.088	1.082	1.089	1.096	1.103	1.111	1.116	1.120
19	1.120	1.119	1.117	1.113	1.110	1.106	1.102	1.099	1.103	1.107	1.111	1.115	1.118	1.120
20	1.120	1.120	1.119	1.117	1.116	1.114	1.113	1.111	1.113	1.115	1.116	1.118	1.119	1.120
21	1.120	1.120	1.120	1.120	1.120	1.120	1.120	1.120	1.120	1.120	1.120	1.120	1.120	1.120

Inhomogeneity profile *edge 3* in IFE, local peak inhomogeneity factor of 1.09

	1	2	3	4	5	6	7	8	9	10	11	12	13	14	15	16	17	18	19	20	21
1	1.090	1.090	1.090	1.090	1.090	1.090	1.090	1.090	1.090	1.090	1.090	1.090	1.090	1.090	1.090	1.090	1.090	1.090	1.090	1.090	1.090
2	1.090	1.090	1.090	1.089	1.089	1.089	1.088	1.088	1.087	1.087	1.086	1.086	1.085	1.085	1.084	1.085	1.086	1.087	1.088	1.089	1.090
3	1.090	1.090	1.089	1.089	1.088	1.087	1.086	1.085	1.084	1.082	1.081	1.079	1.078	1.077	1.075	1.078	1.081	1.084	1.086	1.088	1.090
4	1.090	1.089	1.089	1.087	1.086	1.084	1.083	1.081	1.078	1.076	1.074	1.071	1.068	1.066	1.063	1.069	1.074	1.078	1.083	1.087	1.090
5	1.090	1.089	1.088	1.086	1.083	1.081	1.078	1.075	1.071	1.067	1.063	1.059	1.054	1.050	1.045	1.055	1.063	1.071	1.078	1.084	1.090
6	1.090	1.088	1.085	1.081	1.077	1.072	1.067	1.060	1.053	1.045	1.038	1.029	1.021	1.013	1.003	1.022	1.038	1.053	1.067	1.079	1.090
7	1.090	1.087	1.082	1.076	1.067	1.059	1.050	1.040	1.027	1.014	1.001	0.987	0.973	0.959	0.943	0.975	1.002	1.027	1.050	1.071	1.090
8	1.090	1.085	1.079	1.070	1.058	1.046	1.034	1.019	1.001	0.983	0.965	0.945	0.925	0.905	0.883	0.927	0.966	1.001	1.034	1.064	1.090
9	1.090	1.084	1.075	1.064	1.049	1.034	1.018	0.998	0.975	0.952	0.929	0.902	0.877	0.852	0.823	0.880	0.929	0.976	1.018	1.056	1.090
10	1.090	1.083	1.073	1.059	1.042	1.025	1.006	0.984	0.957	0.930	0.903	0.873	0.844	0.814	0.781	0.847	0.904	0.958	1.007	1.051	1.090
11	1.090	1.082	1.072	1.057	1.039	1.020	1.000	0.976	0.946	0.918	0.889	0.856	0.825	0.792	0.757	0.828	0.890	0.947	1.000	1.048	1.090
12	1.090	1.083	1.073	1.059	1.042	1.025	1.006	0.984	0.957	0.930	0.903	0.873	0.844	0.814	0.781	0.847	0.904	0.958	1.007	1.051	1.090
13	1.090	1.084	1.075	1.064	1.049	1.034	1.018	0.998	0.975	0.952	0.929	0.902	0.877	0.852	0.823	0.880	0.929	0.976	1.018	1.056	1.090
14	1.090	1.085	1.079	1.070	1.058	1.046	1.034	1.019	1.001	0.983	0.965	0.945	0.925	0.905	0.883	0.927	0.966	1.001	1.034	1.064	1.090
15	1.090	1.087	1.082	1.076	1.067	1.059	1.050	1.040	1.027	1.014	1.001	0.987	0.973	0.959	0.943	0.975	1.002	1.027	1.050	1.071	1.090
16	1.090	1.088	1.085	1.081	1.077	1.072	1.067	1.060	1.053	1.045	1.038	1.029	1.021	1.013	1.003	1.022	1.038	1.053	1.067	1.079	1.090
17	1.090	1.089	1.088	1.086	1.083	1.081	1.078	1.075	1.071	1.067	1.063	1.059	1.054	1.050	1.045	1.055	1.063	1.071	1.078	1.084	1.090
18	1.090	1.089	1.089	1.087	1.086	1.084	1.083	1.081	1.078	1.076	1.074	1.071	1.068	1.066	1.063	1.069	1.074	1.078	1.083	1.087	1.090
19	1.090	1.090	1.089	1.089	1.088	1.087	1.086	1.085	1.084	1.082	1.081	1.079	1.078	1.077	1.075	1.078	1.081	1.084	1.086	1.088	1.090
20	1.090	1.090	1.090	1.089	1.089	1.089	1.088	1.088	1.087	1.087	1.086	1.086	1.085	1.085	1.084	1.085	1.086	1.087	1.088	1.089	1.090
21	1.090	1.090	1.090	1.090	1.090	1.090	1.090	1.090	1.090	1.090	1.090	1.090	1.090	1.090	1.090	1.090	1.090	1.090	1.090	1.090	1.090

Inhomogeneity profile *edge 3* in OFE, local peak inhomogeneity factor of 1.09

	1	2	3	4	5	6	7	8	9	10	11	12	13	14
1	1.090	1.090	1.090	1.090	1.090	1.090	1.090	1.090	1.090	1.090	1.090	1.090	1.090	1.090
2	1.090	1.090	1.089	1.088	1.087	1.086	1.085	1.084	1.085	1.086	1.087	1.088	1.089	1.090
3	1.090	1.089	1.087	1.085	1.082	1.080	1.077	1.074	1.077	1.080	1.083	1.086	1.089	1.090
4	1.090	1.088	1.085	1.081	1.076	1.071	1.066	1.061	1.066	1.072	1.077	1.083	1.087	1.090
5	1.090	1.087	1.082	1.075	1.067	1.059	1.051	1.042	1.051	1.060	1.069	1.078	1.086	1.090
6	1.090	1.085	1.075	1.060	1.045	1.030	1.014	0.998	1.015	1.032	1.050	1.068	1.081	1.090
7	1.090	1.081	1.065	1.040	1.015	0.988	0.962	0.934	0.962	0.992	1.021	1.052	1.076	1.090
8	1.090	1.078	1.054	1.019	0.984	0.947	0.909	0.870	0.910	0.951	0.993	1.037	1.070	1.090
9	1.090	1.074	1.044	0.999	0.953	0.905	0.856	0.806	0.858	0.911	0.965	1.021	1.064	1.090
10	1.090	1.072	1.036	0.984	0.931	0.876	0.819	0.761	0.821	0.883	0.946	1.010	1.060	1.090
11	1.090	1.071	1.032	0.976	0.919	0.859	0.798	0.736	0.800	0.866	0.934	1.004	1.057	1.090
12	1.090	1.072	1.036	0.984	0.931	0.876	0.819	0.761	0.821	0.883	0.946	1.010	1.060	1.090
13	1.090	1.074	1.044	0.999	0.953	0.905	0.856	0.806	0.858	0.911	0.965	1.021	1.064	1.090
14	1.090	1.078	1.054	1.019	0.984	0.947	0.909	0.870	0.910	0.951	0.993	1.037	1.070	1.090
15	1.090	1.081	1.065	1.040	1.015	0.988	0.962	0.934	0.962	0.992	1.021	1.052	1.076	1.090
16	1.090	1.085	1.075	1.060	1.045	1.030	1.014	0.998	1.015	1.032	1.050	1.068	1.081	1.090
17	1.090	1.087	1.082	1.075	1.067	1.059	1.051	1.042	1.051	1.060	1.069	1.078	1.086	1.090
18	1.090	1.088	1.085	1.081	1.076	1.071	1.066	1.061	1.066	1.072	1.077	1.083	1.087	1.090
19	1.090	1.089	1.087	1.085	1.082	1.080	1.077	1.074	1.077	1.080	1.083	1.086	1.089	1.090
20	1.090	1.090	1.089	1.088	1.087	1.086	1.085	1.084	1.085	1.086	1.087	1.088	1.089	1.090
21	1.090	1.090	1.090	1.090	1.090	1.090	1.090	1.090	1.090	1.090	1.090	1.090	1.090	1.090

Inhomogeneity profile *edge 3* in IFE, local peak inhomogeneity factor of 1.06

	1	2	3	4	5	6	7	8	9	10	11	12	13	14	15	16	17	18	19	20	21
1	1.060	1.060	1.060	1.060	1.060	1.060	1.060	1.060	1.060	1.060	1.060	1.060	1.060	1.060	1.060	1.060	1.060	1.060	1.060	1.060	1.060
2	1.060	1.060	1.060	1.060	1.059	1.059	1.059	1.059	1.058	1.058	1.058	1.057	1.057	1.056	1.056	1.057	1.058	1.058	1.059	1.059	1.060
3	1.060	1.060	1.059	1.059	1.058	1.058	1.057	1.057	1.056	1.055	1.054	1.053	1.052	1.051	1.050	1.052	1.054	1.056	1.057	1.059	1.060
4	1.060	1.060	1.059	1.058	1.057	1.056	1.055	1.054	1.052	1.051	1.049	1.047	1.046	1.044	1.042	1.046	1.049	1.052	1.055	1.058	1.060
5	1.060	1.059	1.058	1.057	1.055	1.054	1.052	1.050	1.047	1.045	1.042	1.039	1.036	1.033	1.030	1.037	1.042	1.047	1.052	1.056	1.060
6	1.060	1.059	1.057	1.054	1.051	1.048	1.044	1.040	1.035	1.030	1.025	1.019	1.014	1.008	1.002	1.015	1.025	1.035	1.044	1.053	1.060
7	1.060	1.058	1.055	1.050	1.045	1.039	1.034	1.026	1.018	1.009	1.001	0.991	0.982	0.973	0.962	0.983	1.001	1.018	1.034	1.048	1.060
8	1.060	1.057	1.052	1.046	1.039	1.031	1.023	1.013	1.000	0.989	0.977	0.963	0.950	0.937	0.922	0.951	0.977	1.001	1.023	1.043	1.060
9	1.060	1.056	1.050	1.042	1.033	1.022	1.012	0.999	0.983	0.968	0.952	0.935	0.918	0.901	0.882	0.920	0.953	0.984	1.012	1.038	1.060
10	1.060	1.055	1.049	1.040	1.028	1.016	1.004	0.989	0.971	0.954	0.935	0.915	0.896	0.876	0.854	0.898	0.936	0.972	1.004	1.034	1.060
11	1.060	1.055	1.048	1.038	1.026	1.013	1.000	0.984	0.964	0.945	0.926	0.904	0.883	0.862	0.838	0.885	0.926	0.965	1.000	1.032	1.060
12	1.060	1.055	1.049	1.040	1.028	1.016	1.004	0.989	0.971	0.954	0.935	0.915	0.896	0.876	0.854	0.898	0.936	0.972	1.004	1.034	1.060
13	1.060	1.056	1.050	1.042	1.033	1.022	1.012	0.999	0.983	0.968	0.952	0.935	0.918	0.901	0.882	0.920	0.953	0.984	1.012	1.038	1.060
14	1.060	1.057	1.052	1.046	1.039	1.031	1.023	1.013	1.000	0.989	0.977	0.963	0.950	0.937	0.922	0.951	0.977	1.001	1.023	1.043	1.060
15	1.060	1.058	1.055	1.050	1.045	1.039	1.034	1.026	1.018	1.009	1.001	0.991	0.982	0.973	0.962	0.983	1.001	1.018	1.034	1.048	1.060
16	1.060	1.059	1.057	1.054	1.051	1.048	1.044	1.040	1.035	1.030	1.025	1.019	1.014	1.008	1.002	1.015	1.025	1.035	1.044	1.053	1.060
17	1.060	1.059	1.058	1.057	1.055	1.054	1.052	1.050	1.047	1.045	1.042	1.039	1.036	1.033	1.030	1.037	1.042	1.047	1.052	1.056	1.060
18	1.060	1.060	1.059	1.058	1.057	1.056	1.055	1.054	1.052	1.051	1.049	1.047	1.046	1.044	1.042	1.046	1.049	1.052	1.055	1.058	1.060
19	1.060	1.060	1.059	1.059	1.058	1.058	1.057	1.057	1.056	1.055	1.054	1.053	1.052	1.051	1.050	1.052	1.054	1.056	1.057	1.059	1.060
20	1.060	1.060	1.060	1.060	1.059	1.059	1.059	1.059	1.058	1.058	1.058	1.057	1.057	1.056	1.056	1.057	1.058	1.058	1.059	1.059	1.060
21	1.060	1.060	1.060	1.060	1.060	1.060	1.060	1.060	1.060	1.060	1.060	1.060	1.060	1.060	1.060	1.060	1.060	1.060	1.060	1.060	1.060

Inhomogeneity profile *edge 3* in OFE, local peak inhomogeneity factor of 1.06

	1	2	3	4	5	6	7	8	9	10	11	12	13	14
1	1.060	1.060	1.060	1.060	1.060	1.060	1.060	1.060	1.060	1.060	1.060	1.060	1.060	1.060
2	1.060	1.060	1.059	1.059	1.058	1.057	1.056	1.056	1.057	1.057	1.058	1.059	1.060	1.060
3	1.060	1.059	1.058	1.057	1.055	1.053	1.051	1.049	1.051	1.053	1.055	1.057	1.059	1.060
4	1.060	1.059	1.057	1.054	1.051	1.048	1.044	1.041	1.044	1.048	1.052	1.055	1.058	1.060
5	1.060	1.058	1.055	1.050	1.045	1.039	1.034	1.028	1.034	1.040	1.046	1.052	1.057	1.060
6	1.060	1.057	1.050	1.040	1.030	1.020	1.010	0.999	1.010	1.021	1.033	1.045	1.054	1.060
7	1.060	1.054	1.043	1.027	1.010	0.992	0.974	0.956	0.975	0.994	1.014	1.035	1.050	1.060
8	1.060	1.052	1.036	1.013	0.989	0.965	0.939	0.913	0.940	0.967	0.996	1.024	1.046	1.060
9	1.060	1.050	1.029	0.999	0.968	0.937	0.904	0.871	0.905	0.941	0.977	1.014	1.042	1.060
10	1.060	1.048	1.024	0.990	0.954	0.917	0.880	0.841	0.881	0.922	0.964	1.007	1.040	1.060
11	1.060	1.047	1.021	0.984	0.946	0.906	0.866	0.824	0.867	0.911	0.956	1.003	1.038	1.060
12	1.060	1.048	1.024	0.990	0.954	0.917	0.880	0.841	0.881	0.922	0.964	1.007	1.040	1.060
13	1.060	1.050	1.029	0.999	0.968	0.937	0.904	0.871	0.905	0.941	0.977	1.014	1.042	1.060
14	1.060	1.052	1.036	1.013	0.989	0.965	0.939	0.913	0.940	0.967	0.996	1.024	1.046	1.060
15	1.060	1.054	1.043	1.027	1.010	0.992	0.974	0.956	0.975	0.994	1.014	1.035	1.050	1.060
16	1.060	1.057	1.050	1.040	1.030	1.020	1.010	0.999	1.010	1.021	1.033	1.045	1.054	1.060
17	1.060	1.058	1.055	1.050	1.045	1.039	1.034	1.028	1.034	1.040	1.046	1.052	1.057	1.060
18	1.060	1.059	1.057	1.054	1.051	1.048	1.044	1.041	1.044	1.048	1.052	1.055	1.058	1.060
19	1.060	1.059	1.058	1.057	1.055	1.053	1.051	1.049	1.051	1.053	1.055	1.057	1.059	1.060
20	1.060	1.060	1.059	1.059	1.058	1.057	1.056	1.056	1.057	1.057	1.058	1.059	1.060	1.060
21	1.060	1.060	1.060	1.060	1.060	1.060	1.060	1.060	1.060	1.060	1.060	1.060	1.060	1.060